





DISSERTATIONES CHIMICAE UNIVERSITATIS TARTUENSIS

89

**ALEKSANDER TRUMMAL**

Computational Study of Structural and  
Solvent Effects on Acidities of  
Some Brønsted Acids



Institute of Chemistry, Faculty of Science and Technology, University of Tartu,  
Estonia

Dissertation is accepted for the commencement of the Degree of Doctor of  
Philosophy in Physical and Analytical Chemistry on June 25th, 2009 by the  
Doctoral Committee of the Institute of Chemistry, University of Tartu.

Supervisors:            Professor, Dr. Ilmar A. Koppel  
                              Professor, Dr. Peeter Burk  
                              Professor, Dr. Endel Lippmaa

Opponents:            Professor, Dr. Jean-François Gal, Laboratoire de  
                              Radiochimie, Sciences Analytiques et Environnement  
                              (LRSAE), Institut de Chimie de Nice, Université de Nice-  
                              Sophia Antipolis, Nice, France  
                              Professor, Dr. Margus Lopp, Chair of Organic Chemistry,  
                              Department of Chemistry, Tallinn University of  
                              Technology, Tallinn, Estonia

Commencement:      September 22th 2009 at 15:00, 18 Ülikooli St., room 204

Publication of this dissertation is granted by University of Tartu

ISSN 1406–0299  
ISBN 978–9949–19–160–4 (trükis)  
ISBN 978–9949–19–161–1 (pdf)

Autoriõigus Aleksander Trummal, 2009

Tartu Ülikooli Kirjastus  
[www.tyk.ee](http://www.tyk.ee)  
Tellimus nr. 269

# CONTENTS

LIST OF ORIGINAL PUBLICATIONS .....	6
ABBREVIATIONS.....	7
INTRODUCTION.....	8
LITERATURE OVERVIEW .....	10
GOALS OF THE STUDY .....	16
COMPUTATIONAL METHODS .....	17
RESULTS AND DISCUSSION .....	20
CONCLUSIONS .....	46
REFERENCES.....	48
SUMMARY IN ESTONIAN .....	53
ACKNOWLEDGMENTS.....	55
PUBLICATIONS .....	57

## LIST OF ORIGINAL PUBLICATIONS

- I** Peeter Burk, Ilmar A. Koppel, Alar Rummel, and **Aleksander Trummal**. Theoretical Calculation of Intrinsic Acidity and Basicity of FOH. *J. Phys. Chem.* **1995**, *99*, 1432–1435.
- II** Peeter Burk, Ilmar A. Koppel, Alar Rummel, and **Aleksander Trummal**. Can O-H Acid be More Acidic Than Its S-H Analog? A G2 Study of Fluoromethanols and Fluoromethanethiols. *J. Phys. Chem. A* **2000**, *104*, 1602–1607.
- III** Peeter Burk, Uldo Mölder, Ilmar A. Koppel, Alar Rummel, and **Aleksander Trummal**. Theoretical Study of Dimethyl Sulfoxide-Anion Clusters. *J. Phys. Chem.* **1996**, *100*, 16137–16140.
- IV** **Aleksander Trummal**, Alar Rummel, Endel Lippmaa, Peeter Burk, and Ilmar A. Koppel. IEF-PCM Calculations of Absolute  $pK_a$  for Substituted Phenols in Dimethyl Sulfoxide and Acetonitrile Solutions. *J. Phys. Chem. A* **2009**, *113*, 6206–6212.
- V** Peeter Burk, Ivar Koppel, **Aleksander Trummal**, and Ilmar A. Koppel. Feasibility of the Spontaneous Gas-Phase Proton Transfer Equilibria Between Neutral Brønsted Acids and Brønsted Bases. *J. Phys. Org. Chem.* **2008**, *21*, 571–574.

### Author's contribution

- Paper I** Performed some of the theoretical calculations and participated in writing of manuscript.
- Paper II** Performed some of the theoretical calculations and participated in writing of manuscript.
- Paper III** Performed necessary ICR measurements and some of the theoretical calculations, participated in writing of manuscript.
- Paper IV** Corresponding author and main person responsible for planning and writing the manuscript. Performed most of the gas-phase calculations and all calculations of solvation energies and  $pK_a$  values.
- Paper V** Performed some of the theoretical calculations and participated in writing of manuscript.

## ABBREVIATIONS

AIM	Atoms in Molecules
AU	Atomic Units
Alpha	Scaling factor for sphere radius in cavity construction
BDE	Bond Dissociation Energy
COSMO	Conductor-like Screening Model
COSMO-RS	Conductor-like Screening Model for Real Solvents
CPCM	Conductor Polarized Continuum Model
DFT	Density Functional Theory
DMSO	Dimethyl sulfoxide
DPCM	Dielectric Polarized Continuum Model
DPE	Deprotonation Energy
FT-ICR	Fourier Transform Ion Cyclotron Resonance
GA	Gas-Phase Acidity
GB	Gas-Phase Basicity
IC	Isodensity Cutoff value in cavity construction
IEF-PCM	Integral Equation Formalism Polarized Continuum Model
IPCM	Static Isodensity Polarized Continuum Model
MeCN	Acetonitrile
MUE	Mean Unsigned Error
NBO	Natural Bond Orbital
PA	Proton Affinity
PCM	Polarized Continuum Model
RMS	Root Mean Square
SCI-PCM	Self-Consistent Isodensity Polarized Continuum Model
SSC(V)PE	Surface Simulation with Correction for Volume Polarization Electrostatics
TATB	Tetraphenylarsonium tetraphenylborate
Tf	Trifluoromethanesulfonyl group
UA0	United Atom Topological Cavity Model with UFF radii
ZPE	Zero Point Energy correction

## INTRODUCTION

The ability to donate or accept the proton is a fundamental chemical property of a molecule.<sup>1</sup> The acidity or basicity are therefore the important quantitative characteristics of chemical reactivity. A number of processes of great biological and technological relevance (e.g., enzyme catalysis in living organisms, heterogeneous catalysis in oil processing, organic synthesis, etc.) are based on acid-base equilibria. Therefore, the knowledge about acidity and basicity of the reactants and the understanding of the change in their properties upon substitutions or transfer to different solvent systems are prerequisites for the state of the art design of the novel processes for the modern chemical industry.

Traditionally, theoretical chemists use multiparameter correlations to establish conventional descriptors for predicting the influence exerted by different substituents and solvents on major intramolecular structural effects (field-inductive effect, polarizability, hyperconjugation, etc.) responsible for specific acid-base properties of the parent compounds. The advent of powerful multiprocessor computing architectures together with highly sophisticated quantum chemical codes made it possible to perform *ab initio* calculations of acidity and basicity using accurate theoretical methods on reasonably large structures. At the same time quantum chemical calculations provide further data (e.g., electron density and charge distributions, orbital interactions, spectral properties, geometries, etc.) to study relationships between structure and reactivity.

The high electronegativity of the fluorine atom and its ability to create conditions for anionic hyperconjugation<sup>2</sup> made it one of the most simple and important choices among various substituents that strongly affect Brønsted acidity. Therefore, the fluorination of H<sub>2</sub>O, H<sub>2</sub>S, CH<sub>3</sub>OH, and CH<sub>3</sub>SH series of OH and SH acids is expected to raise acidity of these compounds. The systematic high-level investigation of acid-base properties of these compounds and effects of successive fluorination on such properties is carried out in the present study.

Dimethyl sulfoxide (DMSO) and acetonitrile (MeCN) are dipolar aprotic solvents capable of dissolving both hydrophobic and hydrophilic solutes. DMSO is widely used in organic synthesis for rate control of the nucleophilic substitution reactions. MeCN is used as a solvent in the purification of butadiene and in the manufacture of pharmaceuticals. For the modeling of chemical reactions in DMSO and MeCN it is helpful to understand the role of the solvent in complexing a solute molecule or ion and its influence on the acidity or basicity of solutes.

A number of well-established theoretical methods exist for calculating acidities and basicities of isolated molecules in the gas phase. The best of these methods reproduce absolute acidities and basicities well within the acceptable error margins.<sup>3</sup> The situation becomes, however, more complicated when acidity or basicity is calculated for solvated molecules, where the main source of uncertainty stems from the calculation of the energy of solvation. Several theoretical models exist for this case, including supermolecule-style calculations, variants of dielectric continuum theory, and cluster-continuum

approach. The recent review by Tomasi et al.<sup>4</sup> provides extensive coverage of the modern solvation models. Typically, in the case of specific solvation, the dielectric continuum theory is improved by adding solvent molecules explicitly to the solute.<sup>5</sup> However, Liptak et al.<sup>6</sup> demonstrated an outstanding performance of the pure dielectric continuum theory applied to aqueous solutions with much stronger hydrogen bond interactions than in DMSO. In the present study we use supermolecule approach to investigate the structural chemistry of DMSO–anion clusters and dielectric continuum theory to calculate  $pK_a$  values of substituted phenols in DMSO and MeCN solutions.

The dissociation of Brønsted acids in solution occurs due to solvation that provides the energy required to stabilize ion pairs or even completely separated ions. The similar stabilization could take place in the presence of additional charged particles or ionizing radiation. However, the spontaneous proton transfer is expected to occur if sufficiently strong neutral acid encounters the neutral base of a matching strength in a gas phase. One of the goals of the present study is to demonstrate the possibility and understand the mechanism of such spontaneous proton transfer in the gas phase.

# LITERATURE OVERVIEW

## I. Acidity Trends upon Successive Fluorination of OH and SH Acids

It has been known since the time of Moissan<sup>7</sup> that fluorine reacts vigorously with water. The principal products of this reaction are usually HF, O<sub>2</sub>, H<sub>2</sub>O<sub>2</sub>, and OF<sub>2</sub>.<sup>8</sup> In the early 1930s, it was claimed by Dennis and Rochow<sup>9,10</sup> that they succeeded in liberating hypofluorous acid from the solutions of oxy salts of fluorine made by passing F<sub>2</sub> into aqueous alkali followed by neutralization of the excess alkali. However, the unambiguous confirmation of the existence of FOH came only in 1968 in the work of Noble and Pimentel, who isolated it in a solid N<sub>2</sub> matrix at 14–20 K.<sup>11</sup> Later it was discovered that FOH plays the key role of an intermediate in the interaction of F<sub>2</sub> with water.<sup>12</sup> Besides that, the electronic structure and reactivity of this molecule have attracted the attention of theoretical chemists because of the presence of the highly electronegative F atom and the effect of the lone pair-lone pair interactions of adjacent oxygen and fluorine atoms in the relatively small (one hydrogen and two heavy atoms) molecule.

During the last forty years, FOH was experimentally characterized by its microwave spectra,<sup>13</sup> IR spectra in the gas phase,<sup>14</sup> in the nitrogen and argon matrixes,<sup>15</sup> and in the solid state,<sup>16</sup> Raman spectra,<sup>17</sup> photoelectron spectra,<sup>18</sup> and reactivity.<sup>12</sup> An excellent review of the earlier studies of the chemistry and physics of this molecule can be found in ref 19. There are numerous papers reporting the quantum chemical investigation of FOH. So the equilibrium structure and anharmonic force-field constants,<sup>20,21</sup> the energy of its ground state and homolytical dissociation,<sup>21,22</sup> rotational and vibrational spectra,<sup>23</sup> and gas-phase acidity and basicity<sup>24–26</sup> have been calculated. However, no high-level calculations or experimental work on the acid-base properties of FOH were performed when the present study was started. As a rule, the existing empirical predictions of these quantities are at variance with each other as well as with those calculated from the existing thermochemical data. So the gas-phase acidity of FOH could be predicted on the basis of the multiparameter correlation equation to be 362 kcal/mol,<sup>27</sup> from which the proton affinity of around 369 kcal/mol could be estimated. Thermochemical estimates of the proton affinity of FO<sup>-</sup> on the basis of the existing thermochemical data on the FOH molecule [ $\Delta H_f(\text{FOH})$  (-23.0 kcal/mol<sup>28</sup> or -19.9 kcal/mol<sup>22</sup>),  $D(\text{FO-H}) = 98.5$  kcal/mol<sup>28</sup>] and suggested electron affinities of FO<sup>•</sup> (1.4–2.15 eV<sup>29,30</sup>) lead to values in a wide range from 362 to 380 kcal/mol, whereas the most probable value, using  $\text{EA}(\text{FO}^{\bullet}) = 2.15$ ,<sup>30</sup> seems to be in the range 361.8–364.8 kcal/mol. Unfortunately, no experimental data on  $\Delta H_f(\text{FOH}_2^+)$  are available for the thermodynamic estimation of the proton affinity of the neutral FOH molecule.

It is a well-known fact<sup>31</sup> that the acidity of neutral Brønsted acids increases in going down a column of the periodic table, despite the decrease in electronegativity. This behavior is related to the size and polarizability of the species involved and also depends heavily on the bond strength of the X—H group of the acidity center (e.g., O—H, S—H, etc.). Therefore, methanol is less acidic than methanethiol ( $\Delta G_{\text{acid}}$  374.0 kcal/mol<sup>32</sup> and  $\Delta G_{\text{acid}}$  350.6 kcal/mol,<sup>32</sup> respectively), and a similar relationship should also be expected to hold for trifluoromethanol and trifluoromethanethiol.

Trifluoromethanol has attracted considerable interest in recent years as a product of the atmospheric degradation of hydrofluorocarbons and hydrochlorofluorocarbons which contain a CF<sub>3</sub> group.<sup>33</sup> Among other properties the gas-phase acidity of CF<sub>3</sub>OH has also been measured.<sup>34</sup> The reported acidity ( $\Delta G_{\text{acid}}$  323 kcal/mol) is higher than earlier estimations ( $\Delta G_{\text{acid}}$  340 kcal/mol<sup>27</sup>), and even higher than that of CF<sub>3</sub>SH ( $\Delta G_{\text{acid}}$  327.8 kcal/mol<sup>35</sup>). *Ab initio* G2 calculations by Notario et al.<sup>36</sup> seem to support the experimental acidity of CF<sub>3</sub>OH.<sup>34</sup> In effect this means that CF<sub>3</sub>OH should exceed even (CF<sub>3</sub>)<sub>3</sub>COH in acidity ( $\Delta G_{\text{acid}}$  324 kcal/mol<sup>35</sup>). The high acidity of CF<sub>3</sub>OH is especially surprising in view of the fact that the O—H bond in this molecule is reported to be anomalously strong ( $119 \pm 2$  kcal/mol<sup>37</sup>), probably even stronger than the corresponding O—H bond in the water molecule. Both experimental and computational results indicate that the CF<sub>3</sub> group strengthens the O—H bond in CF<sub>3</sub>OH relative to that in CH<sub>3</sub>OH or similar alcohols. The CF<sub>3</sub> group has an apparent  $\beta$ -stabilizing influence in a number of other systems also. For instance, the peroxide linkage in CF<sub>3</sub>OOCF<sub>3</sub> has been measured to be 8 kcal/mol stronger than that of typical alkyl peroxides,<sup>38</sup> and the CF<sub>3</sub>O—OH bond is calculated to be stabilized by 3.5 kcal/mol relative to that of CH<sub>3</sub>O—OH.<sup>39</sup> Similarly, the C—H bond energy in CF<sub>3</sub>CH<sub>3</sub> is about 8.5 kcal/mol greater than that in ethane<sup>38</sup> and the C—H bond in (CF<sub>3</sub>)<sub>3</sub>—CH 8.7 kcal/mol stronger than in (CH<sub>3</sub>)<sub>3</sub>—CH.<sup>40</sup> At the same time, similar to CF<sub>3</sub>OH, (CF<sub>3</sub>)<sub>3</sub>CH also has a surprisingly high acidity ( $\Delta G_{\text{acid}}$  326.6 kcal/mol<sup>35</sup>), which successfully competes with that of (CF<sub>3</sub>)<sub>3</sub>OH ( $\Delta G_{\text{acid}}$  324.0 kcal/mol<sup>35</sup>). While the trend toward the stabilization of  $\beta$  bond energies is evident, the origin of the effect is unclear.

The CF<sub>3</sub> group is well known to bond strongly to adjacent  $\pi$ -donor groups. This ability has been attributed to the negative hyperconjugation effect, or the ability of the formally  $\pi$ -saturated CF<sub>3</sub> group to act as a  $\pi$ -acceptor.<sup>41,42</sup> Wallington et al. have suggested that the effectiveness of negative hyperconjugation in CF<sub>3</sub>OH and CF<sub>3</sub>O radical can account for the anomalously large CF<sub>3</sub>O—H bond strength.<sup>39,43</sup> On the basis of the simple thermodynamic cycle they showed that the anomalously large value for the CF<sub>3</sub>O—H energy can be recast in terms of an anomalously large decrease in C—O bond energy from CF<sub>3</sub>OH to CF<sub>3</sub>O. As an explanation for this large decrease they have proposed that negative hyperconjugation is less effective in stabilizing the CF<sub>3</sub>O radical compared to CF<sub>3</sub>OH, and in this way changes in negative hyperconjugation at the C—O bond ( $\alpha$ -effect) can be manifested in the hydroxyl bond energies ( $\beta$ -effect).

## 2. Effects of Solvation in DMSO and MeCN

**Cluster approach.** The well-known stabilizing nucleophilic solvation in DMSO is based on dimethyl sulfoxide S–O bond oxygen interaction with the solute's electrophilicity center. This interaction favors dissolving MX-type salts due to formation of DMSO–M<sup>+</sup> complex resulting in enhanced reactivity of X<sup>–</sup>.

However, the latest experimental and computational findings confirm also the possibility of electrophilic solvation in DMSO.<sup>44–48</sup> The binding energy in the DMSO-anion clusters may be as high as 30 kcal/mol and may even exceed the stabilizing effect of conventional nucleophilic solvation. Therefore, while considering reactivity in DMSO solutions (e.g., S<sub>N</sub>2-type reactions), the possibility of stabilizing electrophilic solvation should be taken into account.

The first experimental evidence confirming existence of gas-phase clusters between DMSO and the anions dates back to 1984–86. Kebarle et al. applied high-pressure mass spectrometry to study the processes of complexation between Cl<sup>–</sup>, Br<sup>–</sup>, I<sup>–</sup>, and DMSO<sup>44</sup> while Sieck reported formation of DMSO – NO<sub>2</sub><sup>–</sup> and DMSO – C<sub>6</sub>H<sub>5</sub>NO<sub>2</sub><sup>–</sup> clusters.<sup>48</sup> In both studies experimental values of the free energy of complexation were also determined.

In our earlier FT-ICR study<sup>49</sup> we applied the combination of strong magnetic field (4.7 T) and low partial pressure of the reactants (10<sup>–7</sup> mbar) to confirm formation of stable clusters between DMSO and CH<sub>3</sub>O<sup>–</sup>, Cl<sup>–</sup>, and NO<sup>–</sup> anions. At the same time we carried out HF/3–21+G\* calculations to determine the energy of complexation for DMSO – F<sup>–</sup>, DMSO – Cl<sup>–</sup>, DMSO – HO<sup>–</sup>, DMSO – CH<sub>3</sub>O<sup>–</sup>, DMSO – NO<sup>–</sup>, and DMSO – NO<sub>2</sub><sup>–</sup> structures. The calculated energies were in the range of 18.5 kcal/mol (for Cl<sup>–</sup> complex) to 32.6 kcal/mol (for HO<sup>–</sup> complex) and consequently, the stabilizing interaction was verified to be operative in all the structures under investigation.

The researchers provide rather different explanations about the intrinsic nature of this stabilizing interaction. Kebarle et al. explained this interaction as purely electrostatic, i.e., charge (anion) – dipole (DMSO, mainly the S–O bond) interaction, using strong polarization of S–O bond upon complexation and structural features permitting anion access as the main evidence.<sup>44,45</sup> Similar conclusion was obtained even earlier by Koppel based on STO-3G\* ja 3–21G\* *ab initio* calculations.<sup>46,47</sup> Later, Brown, on the basis of solid state X-ray spectroscopy data, proposed that DMSO can bond to anions by forming hydrogen bond between its methyl hydrogen and free electron pair in anion.<sup>50</sup> The co-existence of ion-dipole interactions and hydrogen bonding in similar systems has been discussed and quantitatively analyzed by means of correlation analysis techniques by Abboud et al.<sup>51</sup> This uncertainty has motivated us to further investigate the nature of bonding between DMSO and the anions.

**PCM approach.** The use of various forms of the polarized continuum model (PCM) in addition to cluster approach has become increasingly popular in recent years in studying effects of solvation. Particularly, the results of pK<sub>a</sub> calculations in H<sub>2</sub>O and DMSO/MeCN solutions are presented below.

**Case of H<sub>2</sub>O.** Liptak et al.<sup>6</sup> achieved promising results (accuracy within 0.4–0.5 p*K*<sub>a</sub> units) with the CBS-QB3/CPCM method for carboxylic acids and substituted phenols in water. Murłowska and Sadlej-Sosnowska<sup>52</sup> followed the procedure proposed by Liptak et al. on tetrazoles and achieved a similar precision of 0.4 p*K*<sub>a</sub> units. Da Silva et al.<sup>53</sup> used a combination of high-accuracy gas-phase methods and DPCM solvation procedure to calculate p*K*<sub>a</sub> of HNO<sub>2</sub>. The error margin was below 0.2 p*K*<sub>a</sub> units. Kallies and Mitzner<sup>54</sup> studied aqueous solutions of aliphatic, alicyclic, and aromatic amines with DFT/SCI-PCM combination. The standard deviation of the calculated p*K*<sub>a</sub> values amounted to 0.7 p*K*<sub>a</sub> units. All these calculations employed an absolute thermodynamic cycle, whereas in the following references the relative thermodynamic cycle was applied. Takano and Houk<sup>55</sup> compared CPCM with other methods for calculating aqueous p*K*<sub>a</sub> values. They found that the mean absolute deviation for CPCM is close to the cluster-continuum approach, within 2.19 and 2.06 p*K*<sub>a</sub> units, respectively. Gutowski and Dixon<sup>56</sup> calculated p*K*<sub>a</sub> values of some very strong acids using G3(MP2) and Cosmo solvation procedure with the error margin of ±2 p*K*<sub>a</sub> units. Pliego and Riveros<sup>57</sup> used a cluster/IPCM method to calculate p*K*<sub>a</sub> values of various acids and achieved a precision of 2.2 p*K*<sub>a</sub> units. Klamt et al.<sup>58</sup> used COSMO-RS, combining dielectric continuum theory with a statistical thermodynamics treatment to predict p*K*<sub>a</sub> values of organic and inorganic acids. The error of 0.5 p*K*<sub>a</sub> units is reported to measure rms deviation between p*K*<sub>a</sub> estimates from linear regression and corresponding experimental values. Chipman calculated p*K*<sub>a</sub> values of several acids and bases in water, dimethyl sulfoxide, and acetonitrile from an absolute cycle and surface simulation with correction for volume polarization SSC(V)PE procedure.<sup>59</sup> For bases in the water medium, the results were reasonable with error about 2 p*K*<sub>a</sub> units. For acids, however, the predictive power of the method in water was unsatisfactory.

**Case of DMSO/MeCN.** Almerindo et al.<sup>60</sup> applied PCM with their own parametrization when calculating p*K*<sub>a</sub> values of organic acids in a DMSO solution with rms error of 2.2 p*K*<sub>a</sub> units. Qi et al.<sup>61</sup> calculated p*K*<sub>a</sub> values for transition-metal hydrides in MeCN with precision of 1.5 p*K*<sub>a</sub> units by exploiting sophisticated ONIOM partitioning and CPCM. Klamt et al.<sup>58</sup> calculated p*K*<sub>a</sub> values for seven acids with an rms error of 1.76 p*K*<sub>a</sub> units and low regression slope value (0.70) in DMSO with the COSMO-RS procedure. Eckert et al.<sup>62</sup> also used COSMO-RS to calculate p*K*<sub>a</sub> values for different classes of organic acids in MeCN. The authors reported an rms error of 1.38 p*K*<sub>a</sub> units for the entire data set after uniform correction was added to the calculated values of  $\Delta G_{\text{diss}}$  for compounds forming anions with the localized charge. Kovačević and Maksić<sup>63</sup> applied a combination of DFT and IPCM to calculate p*K*<sub>a</sub> values for various superbases in acetonitrile with the mean absolute deviation of 0.4 p*K*<sub>a</sub> units. The theoretical p*K*<sub>a</sub> values in the work of Klamt et al. and Kovačević and Maksić were calculated by using linear regression fit of either  $\Delta G$  of the acid dissociation reaction (Klamt et al.) or proton affinity of the base (Kovačević and Maksić) with

the experimental  $pK_a$  values. Magill et al.<sup>64</sup> combined CBS-QB3 and CPCM to calculate  $pK_a$  for nucleophilic carbenes in water, DMSO, and MeCN from the absolute thermodynamic cycle. The errors for the two compounds with known experimental values in DMSO were 0.1 and 0.5  $pK_a$  units, respectively. Chipman's SSC(V)PE results for DMSO and MeCN are very encouraging.<sup>59</sup> For DMSO and MeCN, the errors of the  $pK_a$  values, measured as deviations between the estimate from linear regression and corresponding experimental value, remain in the range of 0.3–0.6 and 0.1–0.7  $pK_a$  units, respectively. However, the precision of calculated  $pK_a$  depends not only on the theoretical method and the basis set chosen for calculation, but also upon the chosen electron isodensity contour value. Our preliminary experience with SCI-PCM,<sup>65</sup> another continuum solvation method based on isodensity contour for cavity construction, was rather unsuccessful. The mean unsigned error of  $pK_a$  values for the series of substituted phenols in DMSO was 1.88  $pK_a$  units at the B3LYP/6–311+G\*\* level. The analysis of solvation energy dependence on the value of isodensity cutoff revealed significant deficiency of the method, which is caused by uncompensated charge escape from the solute cavity in case of anions. This deficiency seems to be responsible for the low slope value of the linear regression between the calculated and experimental  $pK_a$  values.

Fu et al.<sup>66</sup> presented several protocols to calculate  $pK_a$  values in DMSO and MeCN. Initially, the PCM-based cluster-continuum approach was used to calculate  $pK_a$  values of organic acids in DMSO with a precision of 1.7–1.8  $pK_a$  units. In the follow up, an improved method based on pure integral equation formalism PCM (IEF-PCM) results with UA0 cavity model combined with B3LYP/6–311++G(2df,2p) gas-phase acidities predicted experimental  $pK_a$  values with the errors having standard deviation of 1.4  $pK_a$  units. For MeCN, DPCM solvation method with Bondi cavity was selected to complement B3LYP/6–311++G(2df,2p) gas-phase acidities. The standard deviation of the resulting  $pK_a$  errors was 1.0  $pK_a$  units. It is important to note that authors optimized the cavities for organic solvents, using nondefault scaling factors applied to the atomic radii. The values of 1.1 and 1.2 for DMSO and MeCN, respectively, resulted in the lowest standard deviation and the highest correlation coefficient.

For several types of cavity models, including UA0 and Bondi, the default scaling factors are specifically optimized for aqueous solutions. The results of Fu et al. confirm the requirement of cavity tuning as a prerequisite for calculation of solvation free energies in organic solvents.

The analysis of reference data suggests that integral equation formalism PCM,<sup>67</sup> the latest formulation of PCM model with carefully adjusted solute cavities, could be the method of choice (along with equivalent SSC(V)PE) if one is interested in absolute  $pK_a$  calculations in DMSO and MeCN with the precision close to 0.5  $pK_a$  units, an important benchmark established for aqueous solutions. It is worth mentioning that both IEF-PCM and SSC(V)PE provide proper treatment of volume polarization, which is absolutely essential for  $pK_a$  calculation of neutral acids.

### 3. Spontaneous Proton Transfer in the Gas Phase

The currently existing experimental gas-phase scale of Brønsted acidities (GA) of neutral acids covers the over 130 kcal/mol range from ethane (GA=411.7 kcal/mol) and its derivatives to (n-C<sub>4</sub>F<sub>9</sub>SO<sub>2</sub>)<sub>2</sub>NH (GA=284.1 kcal/mol).<sup>35a,68</sup> In a recent series of papers it was suggested that even much higher acidities (close to 200 kcal/mol) could be expected for some modern neutral superacids.<sup>69-74</sup>

The intrinsic basicity scale of the gas-phase Brønsted basicities (GB) covers the range between GB=35.5 kcal/mol for helium and GB=264.6 kcal/mol for EtN=P(NMe<sub>2</sub>)<sub>2</sub>NP(NMe<sub>2</sub>)<sub>3</sub>.<sup>75,76</sup> The somewhat outdistanced and not continuously covered region of very high basicity ranges up to 337.5 kcal/mol (Cs<sub>2</sub>O) and is so far represented with experimentally determined values for such superbases as alkali metal hydroxides, alkali metal oxides, alkali metals, and oxides of alkaline earth metals.<sup>77-80</sup> Extremely strong basicities (ranging from *ca* 240 kcal/mol to *ca* 340 kcal/mol) were predicted for families of ylides, imides, phosphazenes, phosphines, and alkali metal nitrides.<sup>71,76,81-85</sup>

This means that the overlap-area for the basicities of neutral and anionic bases (or the acidities of cationic and neutral Brønsted acids) covers more than 130 kcal/mol range from *ca* 200–230 kcal/mol (acidities of CB<sub>11</sub>F<sub>12</sub>H and CB<sub>11</sub>(CF<sub>3</sub>)<sub>12</sub>H)<sup>69</sup> to *ca* 340 kcal/mol (basicities of Cs<sub>2</sub>O<sup>77,80</sup> and K<sub>3</sub>N<sup>83</sup>).

Therefore, the realization of the idea<sup>69,70,83,86,87</sup> of spontaneous (without the presence of solvent, additional charged reactants, or applying ionizing radiation, etc.) gas-phase proton-transfer equilibrium between neutral Brønsted acids and neutral base with similar or overlapping values of gas-phase acidity and gas-phase basicity seems to have waited for a practical solution. Some possible ways of its accomplishment have been proposed.<sup>69,80,83-93</sup>

## GOALS OF THE STUDY

The major goals of the present study are:

- high-level *ab initio* investigation of the influence of the structural factors (the presence of the highly electronegative F atom and the lone pair – lone pair interactions of the adjacent oxygen and fluorine atoms) on the acidity and basicity of FOH
- G2 study of the acidities of  $\text{CH}_{3-n}\text{F}_n\text{OH}$  and  $\text{CH}_{3-n}\text{F}_n\text{SH}$  ( $n = 0-3$ ) families and identification of the key factors responsible for the behavior of the geometries and energetics of these species and their heterolytic and homolytic dissociation products
- theoretical investigation of the nature of bonding in DMSO – anion complexes and obtaining structural information about such complexes
- critical performance test of the IEF-PCM solvation procedure as implemented in Gaussian03 on calculating absolute  $\text{p}K_a$  values of substituted phenols in dimethyl sulfoxide and acetonitrile
- theoretical investigation of interactions of a strong base ( $\text{K}_2\text{O}$ ) with acids of different strength ( $\text{HClO}_4$ ,  $\text{HCl}$ , and  $\text{HF}$ ), and strong acid ( $\text{HClO}_4$ ) with bases ranging from  $\text{K}_2\text{O}$  (GB=322.8 kcal/mol) to  $\text{H}_2\text{O}$  (GB=157.6 kcal/mol) regarding the nature and extent of proton transfer between those partners.

## COMPUTATIONAL METHODS

All *ab initio* quantum chemical computations<sup>94</sup> reported in this study were carried out using Gaussian<sup>95</sup> series of programs.

The neutral, protonated and deprotonated forms of FOH molecule were fully optimized at Hartree–Fock level using the STO-3G, 3–21G, 3–21+G, 6–31G, 6–31G\*, 6–31G\*\*, and 6–31++G\*\* basis sets. With the 6–31G\* basis set, post-Hartree–Fock level (MP2, second-order Møller–Plesset perturbation theory; CISD, configuration interaction with inclusion of singles and doubles) calculations with geometry optimizations were also carried out. G1<sup>96</sup> and G2<sup>97</sup> calculations of energies of the above-mentioned species were performed.

Geometries of the CH<sub>3-n</sub>F<sub>n</sub>OH and CH<sub>3-n</sub>F<sub>n</sub>SH (*n*=0–3) molecules and of the corresponding anions and radicals were fully optimized at the HF/6–31G\* and MP2/6–31G\* levels. Harmonic frequencies were calculated at the HF/6–31G\* level of theory. G2 energies (at 0 K), enthalpies and Gibbs free energies (both at 298.15 K) were also calculated.

Geometries and total energies of DMSO–anion clusters, DMSO molecule, and corresponding anions were calculated at MP2/6–31+G\* and B3LYP/6–31+G\* (Becke’s three-parameter functional<sup>98</sup> is the hybrid method which includes a mixture of Hartree–Fock exchange term with DFT exchange–correlation terms and the nonlocal correlation term provided by the Lee, Yang, and Parr functional<sup>99–101</sup>) levels of theory. All geometries were fully optimized.

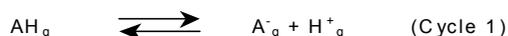
The geometries of substituted phenols and corresponding phenoxide anions were fully optimized at B3LYP/6–311+G\*\* level of theory, and the values of Gibbs free energy were calculated for the standard state of 1 atm at 298.15 K. The second set of acidity values was based on B3LYP/6–311++G(2df,2p) single-point energies computed for B3LYP/6–311+G\*\* optimized structures and corresponding B3LYP/6–311+G\*\* thermal corrections. Finally, the B3LYP/6–311+G\*\* gas-phase acidities were scaled according to the correlation with experimental acidities established previously<sup>102</sup> for the substituted phenols to produce the third set of gas-phase acidity values:

$$\Delta G_{\text{scaled}} = (\Delta G + 34.2) / 1.091$$

For strong acids, bases, and their respective complexes participating in the spontaneous gas-phase proton transfer equilibria DFT calculations with B3LYP hybrid functional were used. Full geometry optimizations and frequency calculations with vibrational analysis were performed using the 6–311+G\*\* basis set. Calculated unscaled frequencies were used to obtain the thermodynamic parameters (at 298.15 K) using the standard procedures.

All stationary points were verified by vibrational analysis to be true minima on the potential energy surface (Nimag=0).

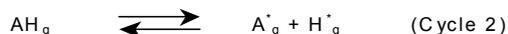
The gas-phase deprotonation energies (DPE) were calculated as the energy change of the following equilibrium at 0 K:



$$\text{DPE} = E(\text{A}^-_g) + E(\text{H}^+_g) - E(\text{AH}_g)$$

The corresponding gas-phase deprotonation enthalpies ( $\Delta H_{\text{acid}}$ ) and acidities ( $\Delta G_{\text{acid}}$ ) were calculated (usually at 298.15 K) similarly using thermochemical corrections from frequency calculations. The values of  $E(\text{H}^+_g)$ ,  $H^{298}(\text{H}^+_g)$ , and  $G^{298}(\text{H}^+_g)$  were set to 0.0, 1.48, and  $-6.29$  kcal/mol, respectively.

Homolytic bond dissociation energies (BDE) were calculated as the energy change of the following reaction:



$$\text{BDE} = E(\text{AH}_g) - [E(\text{A}^*_g) + E(\text{H}^*_g)]$$

$\Delta H_{\text{HBD}}$  and  $\Delta G_{\text{HBD}}$  were also calculated (at 298.15 K).

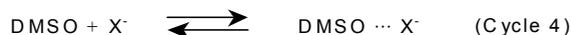
The gas-phase proton affinity (PA) and basicity (GB) were calculated as negative enthalpy and Gibbs free energy change (at 298.15 K) of the reaction



$$\text{PA} = H(\text{B}_g) + H(\text{H}^+_g) - H(\text{BH}^+_g)$$

$$\text{GB} = G(\text{B}_g) + G(\text{H}^+_g) - G(\text{BH}^+_g)$$

The complexation enthalpy was defined by analogy of proton affinities as the negative of the heat of the following reaction:

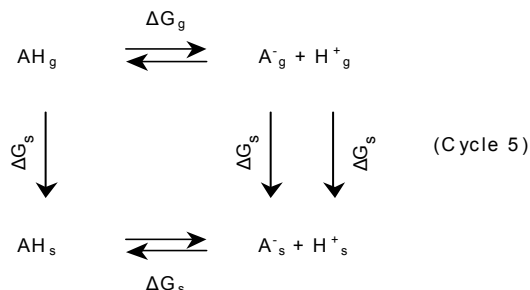


$$\Delta H^{\circ} = E^{\circ}(\text{DMSO}) + E^{\circ}(\text{X}^-) - E^{\circ}(\text{DMSO} \cdots \text{X}^-)$$

where  $E^{\circ}(\text{DMSO})$ ,  $E^{\circ}(\text{X}^-)$ , and  $E^{\circ}(\text{DMSO} \cdots \text{X}^-)$  are total energies of the DMSO molecule, anion, and DMSO–anion complex, respectively. The results of

frequency calculations were used to include ZPE and thermal corrections in the final  $\Delta H^{298}$  values for comparison with the experiment.

Absolute  $pK_a$  calculations are based on the following thermodynamic cycle:



The following relations were applied to calculate  $pK_a$ :

$$K_a = [\text{A}^-_s][\text{H}^+_s] / [\text{AH}_s]$$

$$pK_a = -\log K_a$$

$$\Delta G_s = -RT \ln K_a$$

$$pK_a = \Delta G_s / RT \ln 10$$

$$\Delta G_s = G(\text{A}^-_g) + G(\text{H}^+_g) - G(\text{AH}_g) + RT \ln(24.46) + \Delta G_s(\text{A}^-) + \Delta G_s(\text{H}^+) - \Delta G_s(\text{AH})$$

The  $\Delta G_s$  values in this study were determined from IEF-PCM/B3LYP/6-31+G\*\* single-point calculations on gas-phase B3LYP/6-311+G\*\* optimized geometry with either UA0 (DMSO,  $\alpha=1.1$ ) or Bondi (MeCN,  $\alpha=1.2$ ) cavity in SCFVAC mode using internally stored dielectric constants of 46.7 and 36.64 for dimethyl sulfoxide and acetonitrile, respectively. Both electrostatic and nonelectrostatic (i.e., cavitation, repulsion, and dispersion) terms were included in the calculation of  $\Delta G_s$  values.  $RT \ln(24.46)$  reflects the change in the standard conditions from 1 atm to moles per liter.

Initially,  $\Delta G_s(\text{H}^+)$  was set to  $-268.6$  and  $-252.9$  kcal/mol for DMSO and MeCN, respectively. These values were derived from the free energy of solvation of proton in water as determined by Tissandier et al.<sup>103</sup> ( $-263.98$  kcal/mol) using the tetraphenylarsonium tetraphenylborate (TATB) assumption.<sup>104</sup> Later, the values of  $\Delta G_s(\text{H}^+)$  were adjusted to provide the best correlation between calculated and experimental  $pK_a$  values.

Topological charge density analysis<sup>105</sup> was performed using Bader's PROAIM<sup>106</sup> program package.

Natural bond orbital analysis was based on NBO version 3<sup>107</sup> software.

MOLEKEL<sup>108</sup> software package was used for visualizing electron density and molecular orbitals.

# RESULTS AND DISCUSSION

## I. Acidity Trends upon Successive Fluorination of OH and SH Acids

H<sub>2</sub>O, H<sub>2</sub>S, CH<sub>3</sub>OH, CH<sub>3</sub>SH, and their respective fluorinated derivatives were investigated in the present study to understand relationships between structural factors and geometry and energetics of these OH and SH acids in the gas phase.

**Geometries.** In Table 1.1 are listed the geometries of investigated methanols and methanethiols optimized at the MP2/6–31G\* level of theory. Both mono-fluorinated methanol and methanethiol adopted conformations with OH or SH hydrogen *gauche* to the fluoro substituent (Figure 1.1). The *trans* conformer was not a minimum on the MP2/6–31G\* CH<sub>2</sub>FOH potential energy surface but rather a transition state (5.5 kcal/mol above the minimum) by analogy with fluoromethylamine.<sup>109</sup> Interestingly enough the *cis* (staggered) conformation of CH<sub>2</sub>FOH, which is also a transition state to the rotation around O–H bond, has lower energy (3.0 kcal/mol above the minimum energy *gauche* form). In the case of CH<sub>2</sub>FSH the two corresponding transition states have much closer energies (4.0 and 3.8 kcal/mol above the minimum for *trans* and staggered conformations, respectively).

**Table 1.1.** MP2/6–31G\* Bond Lengths in CH<sub>3-n</sub>F<sub>n</sub>OH and CH<sub>3-n</sub>F<sub>n</sub>SH (*n*=0–3) and the Corresponding Anions and Radicals (Å)

	neutral				anion			radical		
	<i>r</i> C-H	<i>r</i> O-H	<i>r</i> C-O	<i>r</i> C-F	<i>r</i> C-H	<i>r</i> C-O	<i>r</i> C-F	<i>r</i> C-H	<i>r</i> C-O	<i>r</i> C-F
CH <sub>3</sub> OH	1.090	0.970	1.423		1.149	1.323		1.101	1.386	
	1.097							1.096		
	1.097							1.096		
CH <sub>2</sub> FOH	1.089	0.972	1.384	1.390	1.131	1.268	1.559	1.100	1.341	1.384
	1.095							1.100		
CHF <sub>2</sub> OH	1.087	0.976	1.358	1.366	1.117	1.239	1.479	1.098	1.352	1.357
CF <sub>3</sub> OH		0.974	1.350	1.330		1.226	1.431		1.366	1.336
				1.351						1.337
				1.351						1.337
	neutral				anion			radical		
	<i>r</i> C-H	<i>r</i> O-H	<i>r</i> C-O	<i>r</i> C-F	<i>r</i> C-H	<i>r</i> C-O	<i>r</i> C-F	<i>r</i> C-H	<i>r</i> C-O	<i>r</i> C-F
CH <sub>3</sub> SH	1.090	1.340	1.814		1.100	1.826		1.095	1.799	
	1.090							1.090		
	1.090							1.090		
CH <sub>2</sub> FSH	1.091	1.340	1.796	1.389	1.099	1.771	1.444	1.095	1.776	1.363
	1.091							1.095		
CHF <sub>2</sub> SH	1.091	1.341	1.795	1.365	1.098	1.739	1.413	1.094	1.794	1.363
CF <sub>3</sub> SH		1.340	1.797	1.343		1.728	1.388		1.801	1.346
				1.346						1.343
				1.346						1.343

In difluoro-substituted acids the OH and SH hydrogens were also oriented *gauche* relative to both fluoro substituents (Figure 1.1). The *gauche-trans* conformers were local minima on the potential energy surface, but above (by 3.1 kcal/mol for CH<sub>2</sub>FOH and 1.1 kcal/mol for CH<sub>2</sub>FSH) the global *gauche-gauche* minima, and the energy barrier for conversion of the *trans-gauche* conformer into the *gauche-gauche* conformer was found to be small or even negligible (0.1 and 1.3 kcal/mol for CH<sub>2</sub>FOH and CH<sub>2</sub>FSH, respectively).

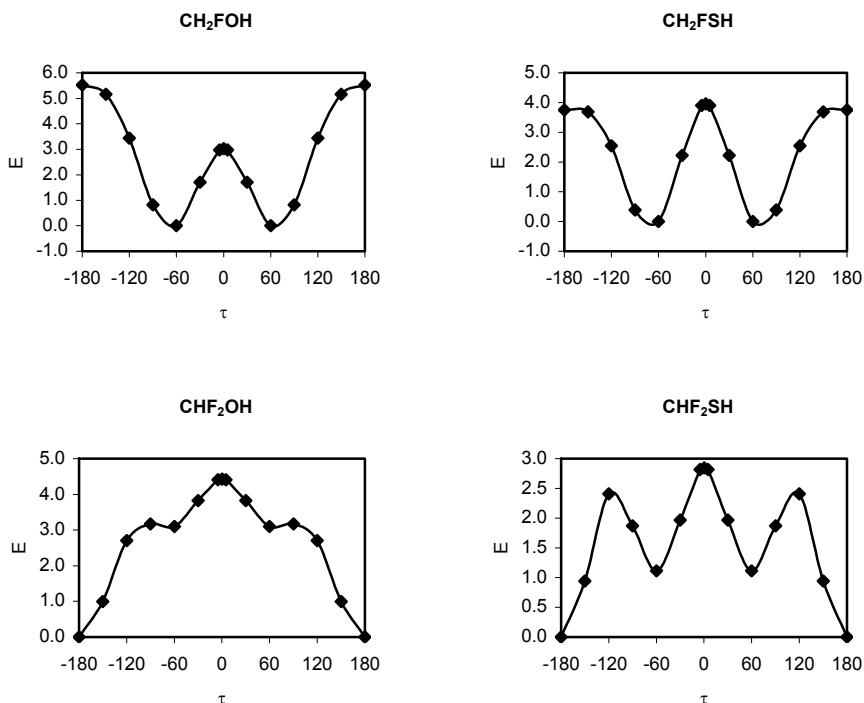


**Figure 1.1.** Energy barriers for rotations around C–O and C–S bonds in CH<sub>2</sub>FOH, CH<sub>2</sub>FSH, CHF<sub>2</sub>OH, and CHF<sub>2</sub>SH. Energies  $E$  are relative to the preferred conformation (kcal/mol).  $\tau$  is the dihedral angle H–O–C–F for CH<sub>2</sub>FOH, H–S–C–F for CH<sub>2</sub>FSH, H–O–C–H for CHF<sub>2</sub>OH, and H–S–C–H for CHF<sub>2</sub>SH.

Such conformational preferences have been observed earlier for substituted methanols<sup>43</sup> and attributed to the hyperconjugative interaction between fluoro substituents and lone pairs of the hydroxyl oxygen. Another possible explanation would attribute such behavior to the electrostatic interaction: the O–H (and also S–H) bond dipoles are oriented opposite those of the CH<sub>2</sub>F and CHF<sub>2</sub> groups, similarly to the orientation of O–H groups in carboxylic acids preferably as *Z* (over *E*).<sup>109</sup> It is clear that electrostatics should be much less important for S–H compounds as the S–H bond dipole moment is much smaller

than that of the O–H bond (due to the smaller electronegativity difference). The distinct differences between potential energy curves for CH<sub>2</sub>FOH and CH<sub>2</sub>FSH, and CHF<sub>2</sub>OH and CHF<sub>2</sub>SH, especially the marked stabilization of the staggered transition state (maximum of the electrostatic stabilization – antiparallel dipole moments) relative to the *trans* form (maximum of electrostatic destabilization – parallel dipole moments) in the case of CH<sub>2</sub>FOH and the absence of a similar effect in the case of CH<sub>2</sub>FSH, indicate that the electrostatic interactions are operative.

Geometries, calculated at the MP2/6–31G\* level (see Table 1.1), indicate that successive fluorine substitution does not affect C–H, O–H, and S–H bond lengths to a considerable extent. The largest geometric changes take place in the C–O and C–F bond lengths in neutral methanols. Upon fluorination the C–O bond in neutral substituted methanols is shortened by 0.040, 0.026, and 0.008 Å, while C–F bond is shortened by 0.024 and 0.015 Å. The C–S bond in methanethiols is shortened by 0.018 Å upon the first fluorine inclusion and remains practically constant upon successive fluorination, thus behaving similarly to the C–H bonds in methanol. These trends are similar to those well-known in the CF<sub>x</sub>H<sub>4-x</sub> series, first noted by Brockway.<sup>110</sup> They have usually been taken as evidence for negative hyperconjugation in CF<sub>x</sub>H<sub>4-x</sub>,<sup>111</sup> but Wiberg<sup>112</sup> and Reed and Schleyer<sup>111</sup> have attributed them to the Coulombic interaction.

In the series of substituted methoxide anions the C–H and especially C–F bonds are longer than their counterparts in neutrals (by 0.03–0.06 and 0.1–0.12 Å, respectively), while the C–O bond is shorter by 0.1–0.12 Å. Successive fluorination leads to the C–H bond being shortened by 0.017 and 0.014 Å, while C–F bonds are lengthened by 0.079 and 0.048 Å. Similarly, the C–H and C–F bonds are longer (compared to those in neutrals) in substituted methylthio anions and the C–S bonds shorter by 0.02–0.07 Å, except for that in CH<sub>3</sub>S<sup>–</sup>, where the C–S bond is 0.012 Å longer than in the neutral. Here the successive fluorination also has the C–H and C–F bond shortening effect, but the changes are smaller (0.0002 and 0.0017 Å for C–H bonds and 0.031 and 0.024 Å for C–F bonds). In contrast, the changes in C–S bond lengths are much more pronounced for anions compared to neutrals, and are 0.054, 0.032, and 0.012 Å.

The C–H bonds *gauche* to the orbital with an unpaired electron are somewhat shorter in methoxy and methylthio radicals compared to methanol and methanethiol, while the *trans* C–H bond is longer compared to the similar bonds (relative to the O–H bond) in methanol and methanethiol. Substitution of hydrogens by fluorines has a very small effect (up to 0.0025 Å for methanols and 0.0047 Å for methanethiols) on C–H bonds. The C–O bond is much shorter in methoxy radical compared to methanol (by 0.038 Å), but still longer than in methoxy anion, while the C–S bond in methylthio radical is 0.015 and 0.026 Å shorter than in methanethiol and methylthio anion, respectively. In all radicals the subsequent inclusion of fluorines leads to the shortening of C–F bonds (by 0.028 and 0.020 Å for methoxy radicals and by 0.024 and 0.020 Å for methylthio radicals). Inclusion of the first fluorine into methoxy and methylthio radicals leads to the marked decrease of the C–O and C–S bonds as in the case

of neutrals and anions. In contrast, the inclusion of the second and third fluorine leads to the lengthening of the corresponding C–O and C–S bonds.

**Energetics.** G2 energies, deprotonation energies, and homolytic bond dissociation energies (at 0 K) are given in Table 1.2. G2 enthalpies, Gibbs energies, acidities, and homolytic bond dissociation enthalpies and Gibbs energies (all at 298.15 K) are given in Tables 1.3 and 1.4 along with experimental gas-phase acidities. In most cases where comparisons are available, the experimental and calculated acidities are in reasonably good agreement (usually within  $\pm 2$  kcal/mol) with each other.

**Table 1.2.** G2 Energies ( $E$ , au), Deprotonation Energies (DPE, kcal/mol), and Homolytic Bond Dissociation Energies (BDE, kcal/mol) at 0K for the Studied OH and SH Acids

	$E(\text{AH})$	$E(\text{A}^-)$	$E(\text{A}^*)$	DPE	BDE
H <sub>2</sub> O	-76.33206	-75.71278	-75.64391	388.6	118.1
FOH	-175.35341	-174.78103	-174.69627	359.2	98.6
CH <sub>3</sub> OH	-115.53490	-114.92709	-114.86753	381.4	105.0
CH <sub>2</sub> FOH	-214.70200	-214.13225	-214.03480	357.5	104.9
CHF <sub>2</sub> OH	-313.87904	-313.33690	-313.19517	340.2	115.4
CF <sub>3</sub> OH	-413.05170	-412.53052	-412.36257	327.0	118.7
H <sub>2</sub> S	-398.93071	-398.37158	-398.28697	350.9	90.2
FSH	-498.05020	-497.50370	-497.41820	342.9	82.8
CH <sub>3</sub> SH	-438.14847	-437.57977	-437.51126	356.9	86.1
CH <sub>2</sub> FSH	-537.30052	-536.75071	-536.66308	345.0	86.3
CHF <sub>2</sub> SH	-636.46412	-635.93207	-635.82135	333.9	89.6
CF <sub>3</sub> SH	-735.63544	-735.11573	-734.99183	326.1	90.1

However, a more noticeable deviation is present in case of CF<sub>3</sub>SH, where the difference between the available experimental acidity value and G2 calculations amounts to more than 6 kcal/mol. Unfortunately, the performance of the G2 theory for reproducing the gas-phase acidities was never checked for relatively more acidic Brønsted acids, and a question of whether any scaling of the directly calculated  $\Delta G_{\text{acid}}$  values is necessary remains unanswered. Therefore, on those grounds it is probably too early to call for the urgent revision of the published experimental value for CF<sub>3</sub>SH. Our experience<sup>113</sup> with G2 calculations of intrinsic acidities of some strong conventional acids (e.g., FSO<sub>3</sub>H) seems to support the necessity of such scaling.

**Table 1.3.** G2 Gibbs Energies ( $G$ , au), Gas-Phase Acidities ( $\Delta G_{\text{acid}}$ , kcal/mol), and Homolytic Bond Dissociation Gibbs Energies ( $\Delta G_{\text{homol}}$ , kcal/mol) for the Studied OH and SH Acids at 298.15K, and the Corresponding Experimental Gas-Phase Acidities ( $\Delta G_{\text{acid}}^{\text{e}}$ , kcal/mol)

	$G(\text{AH})$	$G(\text{A}^-)$	$G(\text{A}^*)$	$\Delta G_{\text{acid}}$	$\Delta G_{\text{acid}}^{\text{e}}$	$\Delta G_{\text{homol}}$
H <sub>2</sub> O	-76.34965	-75.72903	-75.66080	383.4	384.1 <sup>114</sup>	111.2
FOH	-175.37519	-174.80124	-174.71690	354.1	355.6 <sup>115</sup>	92.1
CH <sub>3</sub> OH	-115.55762	-114.94825	-114.89046	376.3	374.0 <sup>32</sup>	97.6
CH <sub>2</sub> FOH	-214.72674	-214.15677	-214.05987	351.6		97.4
CHF <sub>2</sub> OH	-313.90536	-313.36301	-313.22186	334.2		107.9
CF <sub>3</sub> OH	-413.07922	-412.55666	-412.39060	320.9	323.0 <sup>34</sup>	111.1
H <sub>2</sub> S	-398.95022	-398.38943	-398.30545	345.8	344.8 <sup>32</sup>	83.6
FSH	-498.07343	-497.52502	-497.44002	338.0		76.4
CH <sub>3</sub> SH	-438.17269	-437.60233	-437.53554	351.8	350.6 <sup>32</sup>	78.8
CH <sub>2</sub> FSH	-537.32665	-536.77641	-536.68939	339.2		78.9
CHF <sub>2</sub> SH	-636.49183	-635.95927	-635.84926	328.1		82.2
CF <sub>3</sub> SH	-735.66417	-735.14289	-735.02100	321.0	327.8 <sup>35</sup>	82.6

**Table 1.4.** G2 Enthalpies ( $H$ , au), Gas-Phase Deprotonation Enthalpies ( $\Delta H_{\text{acid}}$ , kcal/mol), and Homolytic Bond Dissociation Enthalpies ( $\Delta H_{\text{homol}}$ , kcal/mol) for the Studied OH and SH Acids at 298.15K, and the Corresponding Experimental Gas-Phase Deprotonation Enthalpies ( $\Delta H_{\text{acid}}^{\text{e}}$ , kcal/mol)

	$H(\text{AH})$	$H(\text{A}^-)$	$H(\text{A}^*)$	$\Delta H_{\text{acid}}$	$\Delta H_{\text{acid}}^{\text{e}}$	$\Delta H_{\text{homol}}$
H <sub>2</sub> O	-76.32828	-75.70947	-75.64060	389.8	390.7 <sup>114</sup>	119.3
FOH	-175.34959	-174.77763	-174.69293	360.4	362.5 <sup>115</sup>	99.8
CH <sub>3</sub> OH	-115.53061	-114.92324	-114.86356	382.6	380.6 <sup>32</sup>	106.3
CH <sub>2</sub> FOH	-214.69754	-214.12804	-214.03069	358.8		106.2
CHF <sub>2</sub> OH	-313.87418	-313.33233	-313.19067	341.5		116.6
CF <sub>3</sub> OH	-413.04627	-412.52551	-412.35738	328.3	329.8 <sup>34</sup>	120.0
H <sub>2</sub> S	-398.92691	-398.36828	-398.28367	352.0	350.7 <sup>32</sup>	91.4
FSH	-498.04631	-497.50027	-497.41482	344.1		84.0
CH <sub>3</sub> SH	-438.14389	-437.57575	-437.50710	358.0	357.6 <sup>32</sup>	87.3
CH <sub>2</sub> FSH	-537.29564	-536.74635	-536.65872	346.2		87.4
CHF <sub>2</sub> SH	-636.45868	-635.92725	-635.81644	335.0		90.7
CF <sub>3</sub> SH	-735.62944	-735.11035	-734.98622	327.2		91.4

Comparison of acidifying effects of fluorine substitution into parent molecules of the studied series, H<sub>2</sub>O and H<sub>2</sub>S, indicates that the substitution of hydrogen for fluorine has a significantly larger acidifying effect (30 kcal/mol) in the case of a water molecule, whereas in the case of dihydrogen sulfide the acidity increase is only 8 kcal/mol. At the same time, it is evident that the two most acidic representatives of the series of fluorine-substituted methanols and methanethiols, respectively, CF<sub>3</sub>OH and CF<sub>3</sub>SH, are predicted by G2 theory to have rather close intrinsic acidity. Indeed, in sharp contrast to, e.g., methanol and metha-

nethiol (the latter is 23.4 kcal/mol more acidic than CH<sub>3</sub>OH) or water and H<sub>2</sub>S (the latter is 39.3 kcal/mol more acidic than H<sub>2</sub>O), trifluoromethanol exceeds CF<sub>3</sub>SH in calculated gas-phase acidity by 0.1 kcal/mol at 298 K! It should be noted that at 0 K the CF<sub>3</sub>SH is still predicted to be a stronger acid by 0.8 kcal/mol, and the inversion of the acidity order is due to an entropy factor: on the  $\Delta H_{\text{acid}}$  scale (at 298 K) CF<sub>3</sub>SH is by 1.1 kcal/mol a stronger acid compared to CF<sub>3</sub>OH.

At the same time, the calculated gas-phase acidities for both CF<sub>3</sub>OH and CF<sub>3</sub>SH also exceed the experimentally determined  $\Delta G_{\text{acid}}$  value for (CF<sub>3</sub>)<sub>3</sub>COH (324.0 kcal/mol). The further insight can be obtained by adding the calculated acidity values of (CF<sub>3</sub>)<sub>3</sub>COH and (CF<sub>3</sub>)<sub>3</sub>CSH to the general acidity trend. The G3(MP2) calculations predict  $\Delta G_{\text{acid}}$  values of 324.0 and 314.9 kcal/mol for (CF<sub>3</sub>)<sub>3</sub>COH and (CF<sub>3</sub>)<sub>3</sub>CSH, respectively. The former value matches exactly the experimental acidity value of (CF<sub>3</sub>)<sub>3</sub>COH. For CF<sub>3</sub>OH and CF<sub>3</sub>SH the G3(MP2) acidity values are 321.9 and 321.1 kcal/mol, respectively. Thus, at G3(MP2) level CF<sub>3</sub>SH is by 0.8 kcal/mol stronger acid than CF<sub>3</sub>OH. However, it appears that for CF<sub>3</sub>OH acidity trend is broken and this acid is much stronger than one could expect. The reason behind this enormous acidic strength is extreme anionic hyperconjugation. NBO analysis of orbital interactions at B3LYP/6-311+G\*\* level reveals that in energetic terms CF<sub>3</sub>O<sup>-</sup> is about 3 times more stabilized due to electron density delocalization as compared to CF<sub>3</sub>S<sup>-</sup>. Unlike CF<sub>3</sub>S<sup>-</sup> where the main contributors responsible for stabilization are interactions between sulfur lone pairs and C-F antibonding orbitals, CF<sub>3</sub>O<sup>-</sup> exhibits very strong geminal interactions (E(2) stabilization energy of 1000–1700 kcal/mol) between C-F and O-C antibonding orbitals. It is also worth mentioning that NBO analysis suggests the significant increase in the bond order between carbon and oxygen atoms in CF<sub>3</sub>O<sup>-</sup>. For the (CF<sub>3</sub>)<sub>3</sub>COH and (CF<sub>3</sub>)<sub>3</sub>CSH pair the difference in anionic hyperconjugation is rather small and acidity order is determined mainly by the difference in O-H and S-H bond strength while for CF<sub>3</sub>OH and (CF<sub>3</sub>)<sub>3</sub>COH the stabilizing effect of higher polarizability of C<sub>4</sub>F<sub>9</sub> group prevails.

There is no doubt that CF<sub>3</sub>OH and CF<sub>3</sub>SH play an important role in understanding the influence of substituent effects on the acidity of fluorine-substituted alcohols and thiols. However, the procedures of measurement of their gas-phase acidity are rather complicated, in particular because of the presence of different competing side reactions which are most pronounced in the case of CF<sub>3</sub>OH (elimination of HF, formation of H-bonded complexes with F<sup>-</sup>, etc.). Therefore, an additional careful study, review and verification of the experimental data on the gas-phase acidities of both CF<sub>3</sub>OH and CF<sub>3</sub>SH, seems to be highly desirable.

Inspection of the acidity trends shows (as expected) increased acidity after each successive fluorine introduction. Also, quite logically, each additional replacement of hydrogen by fluorine leads to a smaller acidity increase compared to those of the previous ones. Interestingly, in the case of methanethiol,

the acidifying effects ( $\Delta\Delta G_{\text{acid}}$ ) of the first and second fluorine substitutions are quite close (12.6 and 11.1 kcal/mol), while the third substitution leads to much smaller acidity enhancement (7.1 kcal/mol). The successive fluorine substitutions in methanol lead to a much smoother acidity increase: 24.7, 17.4, and 12.4 kcal/mol, respectively. Therefore, in the case of the series of substituted methanols, the effects are much larger than in methanethiol.

Changes in homolytic bond dissociation energies ( $\Delta\Delta H_{\text{HBD}}$ ) are much more confusing. In both series of substituted methanols and methanethiols, the first fluorine substitution practically does not change the bond dissociation energy, while the second substitution leads to the marked increase of the BDE (10.4 kcal/mol in the case of methanol and 3.3 kcal/mol for methanethiol). The third substitution has a very small effect on the BDE of methanethiol (0.4 kcal/mol). In the case of methanol the effect is 3.4 kcal/mol, which is also considerably smaller than the effect of the second substitution. From these data it is clear that the effect responsible for the BDE increase is not a simple inductive effect as suggested for fluorinated ethanols,<sup>40</sup> where the monotonous (although not quite linear) increase in the BDE with successive replacements of  $\beta$ -hydrogens by fluorine atoms was found.

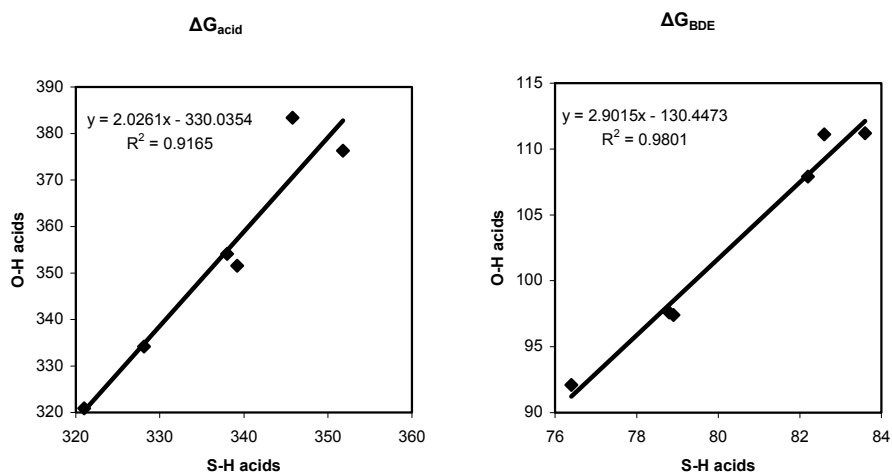


**Figure 1.2.** Correlation between calculated acidities (at 298.15 K) of OH and SH acids, and between calculated bond dissociation free energies (at 298.15 K) of OH and SH acids.

Figure 1.2 presents the relationships between the acidities of investigated O–H and S–H acids, and between homolytic bond dissociation energies of the same compounds. One can see that the structural effects on the acidities and BDEs of both families are linearly related to a high degree of precision ( $R^2 = 0.917$  and  $R^2 = 0.980$ , respectively), while the slopes of correlation lines are significantly larger than 1 (in fact 2.03 and 2.90, respectively). Thus, in accord with the earlier work of Molina et al.,<sup>116</sup> substituent effects are appreciably attenuated in

thiols with respect to alcohols, possibly as a consequence of the S–C bonds being longer than the O–C ones.

Wallington has proposed hyperconjugation as the explanation of BDE trends in fluoromethanols. He argues that a single fluorine substituent can have a hyperconjugative interaction only with one free electron pair on oxygen, thus stabilizing both CH<sub>2</sub>FOH and CH<sub>2</sub>FO radical to the same extent (as both species have an oxygen lone pair available). In contrast, he writes<sup>43</sup> “Multiple halogen substituents can interact with and stabilize two O  $\pi$ -electron pairs on an adjacent oxygen. Approximately two electron pairs are available in the saturated methanols, but in the methoxy radicals only one pair plus one unpaired electron are available.”

Besides the interactions between fluorine substituents and oxygen, one should also consider the interactions between fluorine atoms in multiply substituted species as it is well known that carbon energetically prefers to be multiply substituted by fluorine.<sup>112</sup> The extra stability of multiply substituted fluoromethanes as compared to the methyl fluoride has also been commonly discussed in terms of negative hyperconjugation.

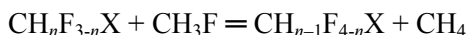
**Table 1.5.** Energetics ( $E_{(1)}$ , kcal/mol) of Stepwise Fluorination by the Isodesmic Reaction  $\text{CH}_n\text{F}_{3-n}\text{X} + \text{CH}_3\text{F} = \text{CH}_{n-1}\text{F}_{4-n}\text{X} + \text{CH}_4$

molecule	$E_{(1)}$ , neutral	$E_{(1)}$ , anion	$E_{(1)}$ , radical
H <sub>2</sub> O	76.6	47.1	57.1
CH <sub>3</sub> OH	-14.9	-38.8	-15.0
CH <sub>2</sub> FOH	-21.1	-38.5	-10.7
CHF <sub>2</sub> OH	-18.4	-31.5	-15.1
H <sub>2</sub> S	15.0	7.1	7.6
CH <sub>3</sub> SH	-5.5	-17.3	-5.3
CH <sub>2</sub> FSH	-12.7	-23.9	-9.4
CHF <sub>2</sub> SH	-17.6	-25.3	-17.0
CH <sub>4</sub>	0.0		
CH <sub>3</sub> F	-12.8		
CH <sub>2</sub> F <sub>2</sub>	-20.2		
CHF <sub>3</sub>	-18.4		

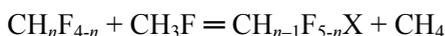
**Table 1.6.** G2 Energies ( $E$ , au) at 0K for Methane and Fluoromethanes

molecule	$E$	molecule	$E$
CH <sub>4</sub>	-40.41086	CHF <sub>3</sub>	-337.89358
CH <sub>3</sub> F	-139.55422	CF <sub>4</sub>	-437.06631
CH <sub>2</sub> F <sub>2</sub>	-238.71798		

The energetic effects of subsequent fluorination can be compared using the energies of the following isodesmic reaction:



where X is OH, SH, O<sup>-</sup>, S<sup>-</sup>, O<sup>·</sup>, or S<sup>·</sup>. Table 1.5 shows that for substituted methanols the inclusion of the second and third fluorine atoms leads to higher stabilization of the molecule as compared to the first fluorine substituent, whereas the second fluorine is the most stabilizing. Interestingly enough, the stabilization energies obtained by stepwise introduction of fluorines into methanol (14.9, 21.1, and 18.4 kcal/mol) are very close to those obtained from the isodesmic reaction



( $1 \leq n \leq 3$ ) for introduction of fluorines into methane (12.8, 20.2, and 18.4 kcal/mol, based on G2(0 K) energies in Table 1.6). As we have similar systems here, and the energy trends are also the same, we expect that the stabilizing mechanism should also be the same for both systems.

In case of substituted methoxy anions the stabilizing energies of fluorine substitution are the largest (up to 38.8 kcal/mol for the first fluorine), and decrease somewhat as the degree of fluorination increases. For methoxy radical the first and third substitutions are energetically practically identical (15.0 and 15.1 kcal/mol, respectively), while the second one is somewhat smaller (10.7 kcal/mol). These energy trends in methoxy radicals contradict the electrostatic model proposed by Wiberg<sup>112</sup> as there should not be any reason for lesser electrostatic stabilization in difluoromethoxy radical compared to trifluoromethoxy radical neither by saturation nor by repulsion between lone pairs of fluorine atoms.

In contrast to substituted methanols, for methanethiol the successive fluorine substitutions stabilize neutrals, anions, and radicals in a synergistic manner, i.e., each successive substitution has more significant stabilization energy. The stabilization energies are greatest for anions as in the case of substituted methanols. The radicals are somewhat less stabilized than neutrals.

One might assume that the change of one H atom in the H<sub>2</sub>O molecule for fluorine should, due to the extremely high electronegativity (field-inductive effect) of the latter, result in a compound, which must be significantly more acidic than water. The counteracting effects on the acidity are expected to be displayed by increased lone pair – lone pair repulsion in the FO<sup>-</sup> anion as compared to the neutral acid, FOH, and by the slightly smaller polarizability of the F atom as compared to the hydrogen atom. Since, in fact, the calculated acidity is much higher for FOH (354.1 kcal/mol) than the corresponding quantity for H<sub>2</sub>O (383.4 kcal/mol), the two latter effects must have much less influence on the acidity of FOH than the first one (i.e., field-inductive effect).

Similarly, the basicity of FOH should be much less than that of H<sub>2</sub>O due to the stronger field-inductive effect and also to the slightly lower polarizability of the F atom. Simultaneously, due to the protonization of FOH, the counteracting base-strengthening effect of the elimination of the adjacent lone pair repulsion should be present. As can be seen from comparison of the proton affinities for H<sub>2</sub>O (166.5<sup>117</sup> kcal/mol) and FOH (135.3 kcal/mol), the first two effects seem to be dominant.

The comparison of the calculated acidity of FOH (354.1 kcal/mol) with the corresponding value for CF<sub>3</sub>OH (320.9 kcal/mol) shows that the latter is more acidic than FOH by *ca* 33 kcal/mol. On the assumption of the roughly similar field-inductive effects of the F atom and CF<sub>3</sub> group<sup>27,118,119</sup> and contribution (*ca* 2.3 kcal/mol<sup>118</sup>) to the stronger acidity of CF<sub>3</sub>OH due to the higher polarizability of the CF<sub>3</sub> group as compared to the fluorine atom, the remaining gap of *ca* 31 kcal/mol could be mainly attributed to the acid-strengthening resonance (anionic hyperconjugation<sup>35b</sup>) effect which accompanies the acidic dissociation of CF<sub>3</sub>OH. Some contribution from destabilizing lone pair – lone pair repulsion effect should be also considered, since in CF<sub>3</sub>OH and its anion there are no lone pairs in the  $\alpha$ -position to the deprotonation center.

As indicated above, the major structural effects responsible for the rather high acidity of CF<sub>3</sub>OH, CF<sub>3</sub>SH, and evidently also (CF<sub>3</sub>)<sub>3</sub>CH are negative (anionic) hyperconjugation and electrostatic effects. In the case of those species the first effect seems to be dominating.

## 2. Effects of Solvation in DMSO and MeCN

**Cluster approach.** Calculated dissociation energies of complexes between DMSO and anions are presented in Table 2.1. Comparison with the available experimental results for the DMSO–Cl<sup>–</sup> complex ( $\Delta H^{298}$  was found to be 18.6, 16.3, and 18.6 kcal/mol by MP2, B3LYP, and experiment,<sup>44</sup> respectively) and the DMSO–NO<sub>2</sub><sup>–</sup> complex (19.5, 17.2, and 19.2 kcal/mol by MP2, B3LYP, and experiment,<sup>48</sup> respectively) indicates good agreement between experiment and calculations. As the primary experimental data are Gibbs energy changes we have also evaluated these quantities for the two complexes above, and once more the agreement between experiment and calculations is good: for the DMSO–Cl<sup>–</sup> complex, the reported<sup>44</sup> experimental  $\Delta G^{298}$  is 12.5 kcal/mol while our calculated values are 12.3 and 10.9 kcal/mol for MP2 and B3LYP. For the DMSO–NO<sub>2</sub><sup>–</sup> complex, the reported<sup>48</sup> experimental  $\Delta G^{420}$  is 8.7 and our calculations give 9.6 and 7.5 kcal/mol for MP2 and B3LYP, respectively. Both methods used give similar results, with B3LYP energies being systematically somewhat lower.

**Table 2.1.** Calculated Total Energies of Monomers  $E_0^x$  and Complexes  $E_0^c$  (au) and Complexation Enthalpies  $\Delta H^\circ$  and  $\Delta H^{298}$  (kcal/mol)

	MP2/6-31+G*				B3LYP/6-31+G*			
	$E_0^x$	$E_0^c$	$\Delta H^\circ$	$\Delta H^{298}$	$E_0^x$	$E_0^c$	$\Delta H^\circ$	$\Delta H^{298}$
DMSO	-552.13005				-553.20011			
F <sup>-</sup>	-99.62385	-651.79998	28.9	28.5	-99.85970	-653.10622	29.1	28.9
Cl <sup>-</sup>	-459.67115	-1011.83196	19.3	18.6	-460.27472	-1013.50165	16.8	16.3
HO <sup>-</sup>	-75.58836	-627.76871	31.6	31.2	-75.79668	-629.04428	29.8	29.6
CH <sub>3</sub> O <sup>-</sup>	-114.74453	-666.92092	29.1	28.0	-115.11531	-668.35294	23.5	23.1
HCOO <sup>-</sup>	-188.71138	-740.87539	21.3	21.0	-189.21950	-742.45036	19.3	19.1
NO <sub>2</sub> <sup>-</sup>	-204.64827	-756.81020	20.0	19.5	-205.16963	-758.39814	17.8	17.2

It has been pointed out in earlier publications<sup>120-122</sup> that the strength of the hydrogen bond (dissociation energy of complex) in the B<sup>-</sup>-HX complexes increases with the basicity of anion. This is true also for data in Table 2.1. The stability order of complexes matches exactly the proton affinity order of anions. Moreover, the correlation between proton affinity and “DMSO affinity” of the anions is remarkable ( $R^2 = 0.967$  for MP2 results and  $R^2 = 0.816$  for B3LYP). This suggests considerable contribution from hydrogen-bond type interaction between DMSO and anion.

**Table 2.2.** Selected Geometrical Parameters of DMSO and Its Complexes with Monodentate Ligands (Bond Lengths in Angstroms and Angles in Degrees)

ligand	MP2/6-31+G*					B3LYP/6-31+G*				
	-	F <sup>-</sup>	Cl <sup>-</sup>	HO <sup>-</sup>	CH <sub>3</sub> O <sup>-</sup>	-	F <sup>-</sup>	Cl <sup>-</sup>	HO <sup>-</sup>	CH <sub>3</sub> O <sup>-</sup>
$r(\text{S-O})$	1.522	1.545	1.540	1.548	1.546	1.519	1.543	1.537	1.545	1.543
$r(\text{S-C})$	1.809	1.798	1.800	1.797	1.798	1.837	1.825	1.828	1.825	1.826
$r(\text{C-H}^1)$	1.094	1.096	1.095	1.096	1.096	1.094	1.097	1.096	1.097	1.097
$r(\text{C-H}^2)$	1.094	1.108	1.098	1.107	1.106	1.095	1.114	1.100	1.112	1.109
$r(\text{C-H}^3)$	1.092	1.093	1.093	1.094	1.094	1.093	1.095	1.094	1.096	1.095
$r(\text{X-S})$		3.434	4.090	3.419	3.425		3.466	4.162	3.459	3.494
$r(\text{X-H}^2)$		1.901	2.520	1.950	1.962		1.850	2.568	1.922	1.959
$\alpha(\text{O-S-C})$	106.7	108.1	107.5	107.6	107.6	106.8	108.6	107.6	108.1	108.0
$\alpha(\text{C-S-C})$	96.3	95.9	96.2	96.4	96.4	96.5	95.7	96.3	96.2	96.2
$\alpha(\text{S-C-H}^1)$	108.9	107.8	108.1	107.8	107.9	109.2	108.0	108.3	107.9	108.0
$\alpha(\text{S-C-H}^2)$	110.1	106.2	108.1	106.9	106.9	109.9	105.8	108.3	106.6	106.8
$\alpha(\text{S-C-H}^3)$	107.3	107.8	107.7	107.5	107.4	106.8	107.7	107.2	107.3	107.3
$\alpha(\text{O-S-X})$		156.3	158.7	158.0	158.3		153.4	158.0	156.0	156.2
$\alpha(\text{C-H}^2\text{-X})$		152.4	157.1	149.3	149.2		154.8	157.2	151.2	151.5

**Table 2.3.** Selected Geometrical Parameters of DMSO and Its Complexes with Bidentate Ligands (Bond Lengths in Angstroms and Angles in Degrees)

ligand	MP2/6-31+G*			B3LYP/6-31+G*		
	-	HCOO <sup>-</sup>	NO <sub>2</sub> <sup>-</sup>	-	HCOO <sup>-</sup>	NO <sub>2</sub> <sup>-</sup>
$r(\text{S-O})$	1.522	1.541	1.539	1.519	1.539	1.537
$r(\text{S-C})$	1.809	1.798	1.799	1.837	1.825	1.826
$r(\text{C-H}^1)$	1.094	1.095	1.095	1.094	1.096	1.096
$r(\text{C-H}^2)$	1.094	1.101	1.099	1.095	1.104	1.102
$r(\text{C-H}^3)$	1.092	1.093	1.093	1.093	1.094	1.094
$r(\text{O}^2\text{-S})$		4.115	4.146		4.526	4.727
$r(\text{X-H}^2)$		2.941	3.102		2.938	3.089
$r(\text{O}^2\text{-H}^2)$		2.104	2.158		2.100	2.156
$r(\text{X-O}^2)$		1.269	1.278		1.260	1.260
$\alpha(\text{O-S-C})$	106.7	107.3	107.3	106.8	107.6	106.1
$\alpha(\text{C-S-C})$	96.3	96.6	96.4	96.5	95.7	96.3
$\alpha(\text{S-C-H}^1)$	108.9	108.1	108.1	109.2	108.4	108.4
$\alpha(\text{S-C-H}^2)$	110.1	109.4	109.1	109.9	109.3	108.9
$\alpha(\text{S-C-H}^3)$	107.3	107.2	107.3	106.8	106.8	107.1
$\alpha(\text{O-S-X})$		154.7	155.4		160.2	159.4
$\alpha(\text{C-H}^2\text{-X})$		156.7	153.8		156.8	160.1
$\alpha(\text{C-H}^2\text{-O}^2)$		175.9	175.2		178.7	179.1
$\alpha(\text{O}^2\text{-X-O}^3)$		129.0	115.4		129.2	116.1
$\alpha(\text{H}^2\text{-O}^2\text{-X})$		119.3	127.1		119.9	127.3

The obtained geometries of complexes are given in Tables 2.2 and 2.3 (numbering of hydrogens is given on Figure 2.1). In all cases complexes preferred  $C_s$  symmetry. Differently from what is reported in earlier studies where diffuse exponents were not included,<sup>44-47</sup> the anions tended not to be on the same line with the O-S bond. They preferred positions in the plane defined by carbons and hydrogens participating in hydrogen bonding (see Figures 2.1 and 2.2). It allows a much shorter distance between the anion and hydrogens of DMSO methyl groups while the distance with S-O bond dipole is increased. Our earlier calculations<sup>49</sup> using 3-21+G\* basis obtained similar trend, and considering good agreement between dissociation energies calculated at both 3-21+G\* and 6-31+G\* levels of theory, and experimental values it is clear that diffuse basis functions are essential for description of the interactions between DMSO and anions. The distances between the anion and adjacent hydrogens in the methyl groups of DMSO are usually between 1.9 and 2.1 Å, which is fairly typical for hydrogen-bonded complexes. The changes in geometry of DMSO upon complex formation are quite small. Most pronounced is the lengthening of S-O bond by 0.02 Å. The C-H bond, which should participate in hydrogen bonding, lengthens only very slightly (about 0.01 Å at the MP2 level of theory).

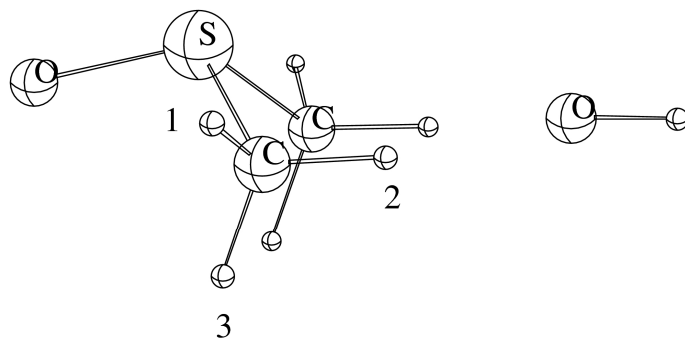


**Figure 2.1.** Structure of the complex between DMSO and monodentate anion ( $\text{OH}^-$ ) and the numbering of hydrogens in the DMSO methyl groups.

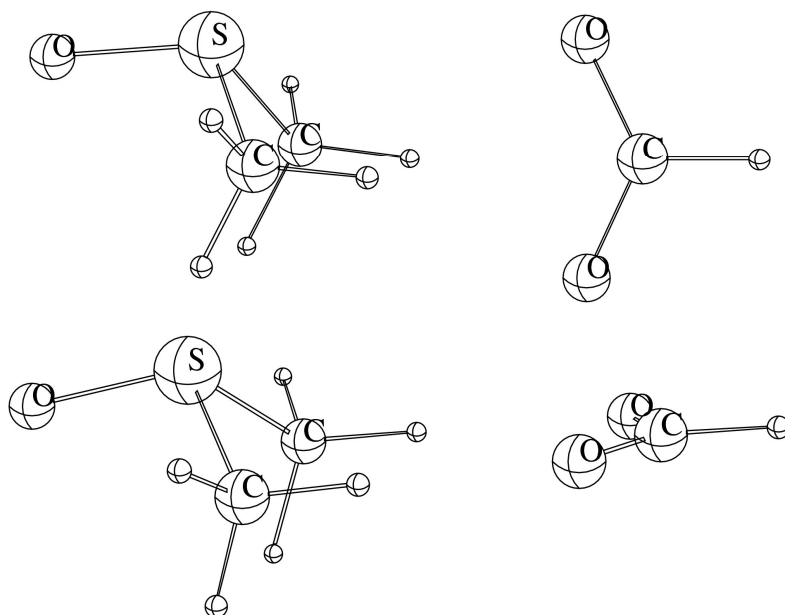


**Figure 2.2.** Two possible structures of the complex between DMSO and bidentate anion ( $\text{HCOO}^-$ ).

The results of NBO charge distribution analysis for all investigated species are presented in Tables 2.4 and 2.5. It can be seen that charge transfer from anions to DMSO is small but constant (*ca* 0.04 electrons). Following the small charge transfer, the changes in charge distribution within DMSO molecule are also small. There are some common trends, which should be noted. Upon complex formation, the negative charge on oxygen increases while the positive charge on sulfur decreases. The charge distributions, obtained by us, clearly indicate that the interaction between DMSO and anions cannot be explained only as interaction between the S-O bond dipole and a point charge. Our results show

that alongside with the increase of the negative charge on oxygen there is similar rise in the negative charge on carbon atoms and positive charge on potentially hydrogen-bonded hydrogens. It once more suggests considerable contribution from hydrogen bonding to the complexation of anions by DMSO.

**Table 2.4.** NBO Charges of DMSO and Its Complexes with Monodentate Ligands

ligand	MP2/6-31+G*					B3LYP/6-31+G*				
	-	F <sup>-</sup>	Cl <sup>-</sup>	HO <sup>-</sup>	CH <sub>3</sub> O <sup>-</sup>	-	F <sup>-</sup>	Cl <sup>-</sup>	HO <sup>-</sup>	CH <sub>3</sub> O <sup>-</sup>
S	1.307	1.269	1.281	1.272	1.274	1.210	1.168	1.188	1.173	1.176
O	-1.074	-1.124	-1.113	-1.128	-1.125	-0.972	-1.034	-1.021	-1.039	-1.033
C	-0.869	-0.888	-0.874	-0.882	-0.881	-0.895	-0.912	-0.897	-0.904	-0.903
H <sup>1</sup>	0.251	0.222	0.232	0.220	0.222	0.257	0.230	0.240	0.228	0.231
H <sup>2</sup>	0.241	0.347	0.306	0.347	0.337	0.251	0.341	0.306	0.340	0.327
H <sup>3</sup>	0.261	0.221	0.233	0.219	0.221	0.269	0.230	0.242	0.229	0.232
X		-0.950	-0.962	-1.382	-1.092		-0.910	-0.948	-1.356	-0.996
ligand		-0.950	-0.962	-0.953	-0.945		-0.910	-0.948	-0.920	-0.917

**Table 2.5.** NBO Charges of DMSO and Its Complexes with Bidentate Ligands

ligand	MP2/6-31+G*			B3LYP/6-31+G*		
	-	HCOO <sup>-</sup>	NO <sub>2</sub> <sup>-</sup>	-	HCOO <sup>-</sup>	NO <sub>2</sub> <sup>-</sup>
S	1.307	1.277	1.281	1.210	1.182	1.184
O	-1.074	-1.154	-1.113	-0.972	-1.025	-1.021
C	-0.869	-0.878	-0.878	-0.895	-0.900	-0.901
H <sup>1</sup>	0.251	0.227	0.229	0.257	0.236	0.238
H <sup>2</sup>	0.241	0.319	0.311	0.251	0.312	0.302
H <sup>3</sup>	0.261	0.232	0.234	0.269	0.241	0.242
X		0.809	0.411		0.619	0.231
O <sup>x</sup>		-0.907	-0.685		-0.797	-0.579
ligand		-0.960	-0.960		-0.935	-0.926

Inspection of the changes in the frequencies of the C–H<sub>2</sub> bond (see Figures 2.1 and 2.2) valence vibrations also indicates the presence of the hydrogen bonding in studied complexes. The unscaled MP2 frequency of that vibration changes from 3100 cm<sup>-1</sup> (free DMSO) to 2849 cm<sup>-1</sup> (DMSO–MeO<sup>-</sup> complex). The smallest change (by 53 cm<sup>-1</sup>) was found for complex between DMSO and chloride anion. Similar changes were found for B3LYP frequencies.

The inspection of the total electron density for the studied complexes revealed significant concentration of the electron density between oxygen atoms of the anions and hydrogen atoms of the DMSO methyl groups. The similar spatial localization was also found for the bonding molecular orbitals of the appropriate geometry. Therefore, the existence of the hydrogen bonding has correct quantum chemical grounds.

Interesting situation occurs in the structure of potentially bidentate anions where the plane defined by anion is perpendicular to the plane defined by the central atom of anion and carbon atoms of DMSO (Figure 2.2, top conformer). Despite the fact that one of the oxygen atoms of the anion is placed closer to the

methyl hydrogens than the second oxygen atom, the hydrogen bond involving the outer oxygen atom is also present, which is confirmed by spatial localization of the bonding molecular orbital. Naturally, the concentration of electron density on this H-bond is lower if compared with the second H-bond and, therefore, the strength of the hydrogen bonds involving different oxygen atoms is unequal for this structure.

To confirm the existence of a hydrogen bond between the anion and hydrogens of the methyl groups of DMSO the Bader's topological charge density analysis<sup>105</sup> was carried out. In all cases the presence of a bond between the anion and hydrogens of methyl groups of DMSO was verified by finding bond critical point between these atoms. The values of bond-localized electron density were in agreement with the results of visual analysis of molecular orbitals and total electron density.

Comparison of energies and geometries of different complexes between DMSO and monodentate anions reveals that the interaction energy depends on both S-X<sup>-</sup> and H<sub>2</sub>-X<sup>-</sup> distances. So for F<sup>-</sup>, CH<sub>3</sub>O<sup>-</sup>, and Cl<sup>-</sup> the energy order follows the lengths of the H<sub>2</sub>-X<sup>-</sup> bond. The OH<sup>-</sup> anion is exception from this rule, and even as CH<sub>3</sub>O<sup>-</sup> obeys it, the difference in energy between the F<sup>-</sup> and CH<sub>3</sub>O<sup>-</sup> complexes is small (0.5 kcal/mol). For these two complexes somewhat shorter S-X<sup>-</sup> distances should be considered, which can indicate an enhanced dipole-charge interaction. Inspection of NBO charges on the oxygen atom in these anions reveals that this may be the case as the charges are considerably higher (-1.38 and -1.10 in OH<sup>-</sup> and CH<sub>3</sub>O<sup>-</sup>, respectively) than in other two anions (-0.95 and -0.96 in F<sup>-</sup> and Cl<sup>-</sup>, respectively).

Further support of the hypothesis of combined hydrogen bonding and electrostatic interaction between an anion and DMSO dipole can be obtained from the study of potentially bidentate anions, NO<sub>2</sub><sup>-</sup> and HCOO<sup>-</sup>. In both cases the complexes in which both oxygens participate in hydrogen bonding were found to be slightly more stable (by 0.32 and 0.30 kcal/mol for NO<sub>2</sub><sup>-</sup> and HCOO<sup>-</sup>, respectively, at the MP2/6-31+G\* level of theory) than monodentate complexes (see Figure 2.2) despite the fact that in the latter case the anion can approach the S-O bond dipole considerably more close (S-O<sub>anion</sub> distance is 4.11 Å in the bidentate complex and 3.25 Å in the monodentate complex, MP2/6-31+G\* results for HCOO<sup>-</sup>), while the O<sub>anion</sub>-H<sub>2</sub> distance increases only slightly (from 2.104 to 2.370 Å, MP2/6-31+G\* results for HCOO<sup>-</sup>). However, as the energy difference between these two conformers is small despite the significant weakening of hydrogen bond interaction in monodentate complex, the enhanced charge-dipole interaction (much shorter distance between dipole and charge) seems to compensate for most of this weakening. Therefore, one should consider the possibility of combined interactions between anions and DMSO, i.e., both hydrogen bonding and charge dipole interaction.

**PCM approach.** The calculated and experimental gas-phase acidities of substituted phenols are presented in Table 2.6. All calculated values at the B3LYP-6-311+G\*\* level are systematically lower (i.e., more acidic) than the

corresponding experimental values. With the single exception of 2,4-dinitrophenol, the same holds true for B3LYP/6-311++G(2df,2p)//B3LYP/6-311+G\*\* as well. The mean unsigned errors are 4.4 and 2.8 kcal/mol for B3LYP/6-311+G\*\* and B3LYP/6-311++G(2df,2p)//B3LYP/6-311+G\*\*, respectively.

**Table 2.6.** Experimental and Calculated Gas-Phase Acidities. All Values Are Given in kcal/mol

substituted phenols	expt <sup>a</sup>	B3LYP/6-311+G**		B3LYP/6-311++G(2df, 2p)// B3LYP/6-311+G**		B3LYP/6-311+G**, scaled	
		calcd	error	calcd	error	calcd	error
phenol	342.3	339.3	-3.0	340.3	-2.0	342.3	0.0
4-NH <sub>2</sub> -phenol	345.6	342.9	-2.7	344.4	-1.3	345.7	0.1
3-NH <sub>2</sub> -phenol	343.7	341.1	-2.6	342.3	-1.4	344.0	0.3
2-NH <sub>2</sub> -phenol	341.3	337.9	-3.4	338.9	-2.4	341.1	-0.2
4-F-phenol	339.9	336.0	-3.9	337.6	-2.3	339.3	-0.6
2-F-phenol	339.0	335.8	-3.2	337.2	-1.8	339.1	0.1
3-F-phenol	336.8	332.9	-3.9	334.5	-2.3	336.5	-0.3
3-Cl-phenol	335.0	331.0	-4.1	332.3	-2.7	334.7	-0.3
2-NO <sub>2</sub> -phenol	329.5	327.3	-2.2	329.0	-0.6	331.4	1.9
3-NO <sub>2</sub> -phenol	327.5	323.6	-3.9	325.1	-2.4	328.0	0.5
4-CN-phenol	325.3	320.7	-4.6	321.9	-3.4	325.3	0.0
3,4,5-Cl <sub>3</sub> -phenol	323.9	320.5	-3.4	322.1	-1.8	325.1	1.2
4-NO <sub>2</sub> -phenol	320.9	314.7	-6.2	316.3	-4.6	319.8	-1.1
2,4-(NO <sub>2</sub> ) <sub>2</sub> -phenol	308.6	308.3	-0.3	310.4	1.8	313.9	5.3
2,3,4,5,6-F <sub>5</sub> -phenol	320.8	315.7	-5.1	318.8	-2.0	320.7	-0.1
2,4,6-(NO <sub>2</sub> ) <sub>3</sub> -phenol	302.8	293.6	-9.2	296.0	-6.8	300.4	-2.4
4-CF <sub>3</sub> -phenol	330.1	325.2	-4.9	327.1	-3.0	329.4	-0.7
3-CF <sub>3</sub> -phenol	332.4	328.2	-4.2	329.8	-2.6	332.2	-0.2
2-CF <sub>3</sub> -phenol	332.2	327.1	-5.1	328.7	-3.5	331.2	-1.0
3,5-(CF <sub>3</sub> ) <sub>2</sub> -phenol	322.9	318.3	-4.6	320.6	-2.3	323.1	0.2
2,3,4,5,6-(CF <sub>3</sub> ) <sub>5</sub> -phenol	298.7	290.2	-8.5	293.9	-4.8	297.3	-1.4
2,4,6-Tf <sub>3</sub> -phenol <sup>b</sup>	291.8	283.5	-8.3	286.1	-5.7	291.2	-0.6
2,4,6-(FSO <sub>2</sub> ) <sub>3</sub> -phenol		280.2		284.9		288.2	
mean error			-4.4		-2.6		0.0
mean unsigned error			4.4		2.8		0.8
rms error			4.9		3.2		1.4

<sup>a</sup>References 35a, 68, 102. <sup>b</sup> Tf denotes CF<sub>3</sub>SO<sub>2</sub>.

The correlation between experimental and calculated gas-phase acidities resulted in the following equations:

$$\Delta G_{\text{expt}} = 0.9062 \Delta G_{\text{calcd}} + 34.6601, R^2 = 0.9905$$

and

$$\Delta G_{\text{expt}} = 0.9365 \Delta G_{\text{calcd}} + 23.2179, R^2 = 0.9904$$

representing B3LYP/6-311+G\*\* and B3LYP/6-311++G(2df,2p)//B3LYP/6-311+G\*\* methods, respectively. It is evident that B3LYP/6-311++G(2df,2p)//B3LYP/6-311+G\*\* results are closer to the experimental acidity values; however, the value of the slope still deviates from unity. A closer look at individual errors in Table 2.6 reveals that 2,4,6-trinitrophenol, pentakis(trifluoromethyl)phenol, and 2,4,6-tris(trifluoromethanesulfonyl)phenol have the largest errors, which on average are 2 times higher than MUE. These enormous errors for the three outer points of the linear regression lower the value of the slope and together represent the root cause of its deviation from unity. Unfortunately, both B3LYP/6-311+G\*\* and B3LYP/6-311++G(2df,2p)//B3LYP/6-311+G\*\* methods have severe difficulties in predicting the gas-phase acidities of these highly acidic phenols. To resolve this situation, the results of B3LYP/6-311+G\*\* calculations were scaled according to the expected correlation with experimental acidities.

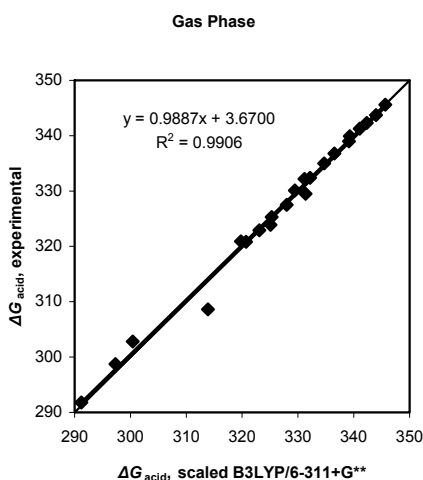


**Figure 2.3.** Correlation between the experimental and calculated gas-phase acidities of phenols in the gas phase (all values in kcal/mol). The  $y=x$  line is added for comparison.

The scaled B3LYP/6-311+G\*\* results predict experimental acidities with the mean unsigned error of 0.8 kcal/mol.

The results of correlation between scaled B3LYP/6-311+G\*\* and experimental gas-phase acidities are presented in Figure 2.3. The slope of the regression line is very close to unity, and the intercept is reasonably small. However, 2,4-dinitrophenol with the error of 5.3 kcal/mol is a clear outlier.

Both B3LYP/6-311++G(2df,2p)//B3LYP/6-311+G\*\* and scaled B3LYP/6-311+G\*\* gas-phase results were used in the following  $pK_a$  calculations. Table 2.7 includes calculated  $pK_a$  values in DMSO with mean unsigned error of 1.2  $pK_a$  units for B3LYP/6-311++G(2df,2p)//B3LYP/6-311+G\*\* results and 1.3  $pK_a$  units for scaled B3LYP/6-311+G\*\* results.

**Table 2.7.** Experimental and IEF-PCM Calculated  $pK_a$  Values in DMSO

substituted phenols	expt <sup>a</sup>	B3LYP/6-311++G(2df,2p)// B3LYP/6-311+G**		B3LYP/6-311+G** scaled		B3LYP/6-311+G** scaled, optimized	
		calcd	error	calcd	error	calcd	error
phenol	18.0	18.0	0.0	19.4	1.4	18.4	0.4
4-NH <sub>2</sub> -phenol	20.8	21.8	1.0	22.8	2.0	21.7	0.9
3-NH <sub>2</sub> -phenol	19.5	19.3	-0.2	20.5	1.0	19.5	0.0
2-NH <sub>2</sub> -phenol	18.2	18.6	0.4	20.2	2.0	19.2	0.9
4-F-phenol	18.0	17.5	-0.5	18.7	0.7	17.7	-0.3
2-F-phenol	15.6	14.8	-0.8	16.3	0.7	15.2	-0.4
3-F-phenol	15.9	15.7	-0.2	17.2	1.3	16.2	0.3
3-Cl-phenol	15.8	15.2	-0.6	16.9	1.1	15.9	0.1
2-NO <sub>2</sub> -phenol	11.0	11.1	0.1	12.9	1.9	11.9	0.9
3-NO <sub>2</sub> -phenol	14.4	12.9	-1.5	15.0	0.6	14.0	-0.4
4-CN-phenol	13.2	11.6	-1.6	14.1	0.9	13.1	-0.1
3,4,5-Cl <sub>3</sub> -phenol	12.6	11.7	-0.9	13.9	1.3	12.9	0.3
4-NO <sub>2</sub> -phenol	10.8	8.3	-2.5	10.8	0.0	9.8	-1.0
2,4-(NO <sub>2</sub> ) <sub>2</sub> -phenol	5.1	4.4	-0.8	7.0	1.9	5.9	0.8
2,3,4,5,6-F <sub>5</sub> -phenol	8.9	7.3	-1.6	8.7	-0.2	7.7	-1.2
2,4,6-(NO <sub>2</sub> ) <sub>3</sub> -phenol	-1.0	-2.3	-1.3	0.9	1.9	-0.1	0.9
4-CF <sub>3</sub> -phenol	14.6	14.0	-0.6	15.7	1.1	14.7	0.1
3-CF <sub>3</sub> -phenol	15.1	14.9	-0.2	16.7	1.6	15.7	0.6
2-CF <sub>3</sub> -phenol	14.4	11.2	-3.2	13.0	-1.4	12.0	-2.4
3,5-(CF <sub>3</sub> ) <sub>2</sub> -phenol	13.2	12.0	-1.2	13.9	0.7	12.8	-0.4
2,3,4,5,6-(CF <sub>3</sub> ) <sub>5</sub> -phenol	3.1	-3.1	-6.2	-0.6	-3.7	-1.7	-4.8
			-1.1		0.8		-0.2
mean error			(-0.8) <sup>b</sup>		(1.0)		(0.0)
			1.2		1.3		0.8
mean unsigned error			(1.0)		(1.2)		(0.6)
			1.8		1.5		1.3
rms error			(1.3)		(1.3)		(0.8)

<sup>a</sup> References 102, 123–128. <sup>b</sup> The values in parentheses exclude 2,3,4,5,6-(CF<sub>3</sub>)<sub>5</sub>-phenol.

To assess performance of theoretical methods, the correlations between calculated and experimental  $pK_a$  values should also be examined. These correlations are characterized by the following parameters:

$$pK_{a \text{ expt}} = 0.8299 pK_{a \text{ calcd}} + 3.1322, R^2 = 0.9627$$

and

$$pK_{a, \text{expt}} = 0.8894 pK_{a, \text{calcd}} + 0.7496, R^2 = 0.9559,$$

based on B3LYP/6-311++G(2df,2p)//B3LYP/6-311+G\*\* and scaled B3LYP/6-311+G\*\* methods, respectively. The regression line slope for both methods is significantly lower than the expected value of 1. This deviation is obviously connected with the large error in  $pK_a$  value of pentakis(trifluoromethyl)phenol. After excluding this compound from the data set, the mean unsigned errors decrease to 1.0 and 1.2  $pK_a$  units for B3LYP/6-311++G(2df,2p)//B3LYP/6-311+G\*\* and scaled B3LYP/6-311+G\*\* methods, respectively, while the corresponding values of the regression line slopes become 0.90 and 0.98. It appears that the former slope value is lower than the latter one because of a rather large error in gas-phase acidity of the picric acid at the B3LYP/6-311++G(2df,2p)//B3LYP/6-311+G\*\* level of theory. The scaled B3LYP/6-311+G\*\* method eliminates that distortion, and the corresponding slope value is very close to unity.

It is also important to note that the value of the intercept strongly depends on the value of the solvation free energy of the proton. The error in this value is a source of systematic error component of the  $pK_a$  series in the case of the slope being close to unity. As solvation free energies of the proton in DMSO and MeCN are estimated from the TATB assumption and are not established thermodynamic values, it is reasonable to optimize these values to minimize the mean unsigned error for the series. It was found that the value of  $-270.0$  kcal/mol for DMSO provides the best fit with the mean unsigned error of 0.6  $pK_a$  units. The corresponding linear regression is presented in Figure 2.4. The work of Westphal and Pliego<sup>129</sup> suggested a more negative value of  $\Delta G_s(H^+)$  in DMSO than the value based on TATB assumption. The solvation free energy of the proton in DMSO has been recently determined from the cluster-pair approach by Kelly et al.,<sup>130</sup> who obtained even more negative value ( $-273.3$  kcal/mol).

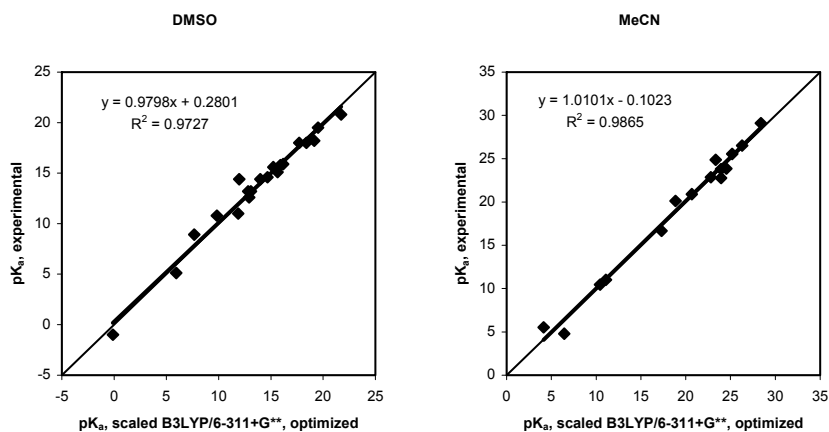


**Figure 2.4.** Correlation between the experimental and calculated  $pK_a$  values of phenols in DMSO. The  $y=x$  line is added for comparison.

The results of  $pK_a$  calculations in MeCN are given in Table 2.8. Unfortunately, there are no experimental  $pK_a$  values available in acetonitrile for many phenols in our series, especially in the less acidic range. Instead, experimental  $pK_a$  values are available for 2,4,6-tris(trifluoromethanesulfonyl)phenol and 2,4,6-tris(fluorosulfonyl)phenol at the acidic end of the scale. The mean unsigned error for the B3LYP/6-311++G(2df,2p)//B3LYP/6-311+G\*\* method is larger for MeCN as compared with that for DMSO, while for the scaled B3LYP/6-311+G\*\* a slight improvement over DMSO results is observed. The regression line slopes are slightly higher as compared to those of DMSO. The resulting equations for B3LYP/6-311++G(2df,2p)//B3LYP/6-311+G\*\* and scaled B3LYP/6-311+G\*\* methods are:

$$pK_{a \text{ expt}} = 0.9522 pK_{a \text{ calcd}} + 3.8261, R^2 = 0.9940$$

and

$$pK_{a \text{ expt}} = 1.0100 pK_{a \text{ calcd}} + 0.6407, R^2 = 0.9864$$

Finally, using previously described arguments, we optimized the value of solvation free energy of the proton for MeCN as done for DMSO. The optimized value of  $-251.9$  kcal/mol resulted in the mean unsigned error of 0.7  $pK_a$  units. The corresponding regression plot is presented in Figure 2.4. Kelly et al.<sup>130</sup> recently determined the solvation free energy of the proton in MeCN from the cluster-pair approach and obtained a more negative value ( $-260.2$  kcal/mol) compared to our optimized value.

**Table 2.8.** Experimental and IEF-PCM Calculated  $pK_a$  Values in MeCN

substituted phenols	expt <sup>a</sup>	B3LYP/6-311++G(2df,2p)// B3LYP/6-311+G**		B3LYP/6-311+G** scaled		B3LYP/6-311+G** scaled, optimized	
		calcd	error	calcd	error	calcd	error
phenol	29.1	26.2	-2.9	27.7	-1.4	28.4	-0.7
2-NO <sub>2</sub> -phenol	22.9	20.3	-2.6	22.1	-0.8	22.8	-0.1
3-NO <sub>2</sub> -phenol	23.9	21.7	-2.1	23.8	-0.1	24.5	0.7
4-CN-phenol	22.8	20.7	-2.1	23.2	0.4	24.0	1.2
4-NO <sub>2</sub> -phenol	20.9	17.4	-3.6	19.9	-1.0	20.7	-0.2
2,4-(NO <sub>2</sub> ) <sub>2</sub> -phenol	16.7	14.0	-2.7	16.6	-0.1	17.3	0.6
2,3,4,5,6-F <sub>5</sub> -phenol	20.1	16.7	-3.4	18.1	-2.0	18.9	-1.3
2,4,6-(NO <sub>2</sub> ) <sub>3</sub> -phenol	11.0	7.2	-3.9	10.4	-0.6	11.1	0.1
4-CF <sub>3</sub> -phenol	25.5	22.8	-2.8	24.5	-1.1	25.2	-0.3
3-CF <sub>3</sub> -phenol	26.5	23.8	-2.7	25.6	-0.9	26.3	-0.2
2-CF <sub>3</sub> -phenol	24.9	20.8	-4.1	22.6	-2.3	23.3	-1.6
3,5-(CF <sub>3</sub> ) <sub>2</sub> -phenol	23.8	21.3	-2.4	23.2	-0.6	23.9	0.2
2,3,4,5,6-(CF <sub>3</sub> ) <sub>5</sub> -phenol	10.5	7.2	-3.3	9.7	-0.8	10.4	0.0
2,4,6-Tf <sub>3</sub> -phenol <sup>b</sup>	4.8	2.0	-2.9	5.7	0.9	6.4	1.6
2,4,6-(FSO <sub>2</sub> ) <sub>3</sub> -phenol	5.5	1.0	-4.6	3.4	-2.1	4.1	-1.4
mean error			-3.1		-0.8		-0.1
mean unsigned error			3.1		1.0		0.7
rms error			3.1		1.2		0.9

<sup>a</sup>References 62, 102, 127, 131. <sup>b</sup>Tf denotes CF<sub>3</sub>SO<sub>2</sub>.

It was also found that an appropriately optimized UA0 cavity model ( $\alpha=1.05$ ) performed less satisfactorily in terms of regression line slope in MeCN than the cavity based on Bondi radii.

Table 2.9 provides comparison of the results of  $pK_a$  calculations from this study with the results published by Eckert et al., Chipman, and Fu et al.

**Table 2.9.** Mean Unsigned Errors (MUE), RMS Errors, Values of Slope, and  $R^2$  Coefficients for the Series of  $pK_a$  Calculations in DMSO and MeCN; IC is Isodensity Cutoff in Atomic Units

methods	DMSO				MeCN			
	MUE	RMS	slope	$R^2$	MUE	RMS	slope	$R^2$
IEF-PCM/B3LYP/6-31+G**// B3LYP/6-311+G**, scaled B3LYP/6- 311+G**//B3LYP/6-311+G** <sup>a</sup>	0.6	0.8	0.980	0.973	0.7	0.9	1.010	0.987
IEF-PCM/B3LYP/6-31+G**// B3LYP/6-31+G*, B3LYP/6- 311++G(2df,2p)//B3LYP/6-31+G* <sup>b</sup>	1.2	1.5	0.893	0.988				
DPCM/B3LYP/6-31+G**// B3LYP/6-31+G*, B3LYP/6- 311++G(2df,2p)//B3LYP/6-31+G* <sup>c</sup>					0.9	0.9	0.791	0.953
DPCM/B3LYP/6-31+G**//B3LYP/ 6-31+G*, B3LYP/6-311++G(2df,2p) //B3LYP/6-31+G* <sup>c,d</sup>					0.8	0.9	0.853	0.937
SSC(V)PE/HF/6-31+G*, IC=0.001 <sup>e</sup>	0.3 <sup>g</sup>		0.764	0.998	0.7 <sup>g</sup>		0.904	0.978
SSC(V)PE/B3LYP/aug-cc-pVTZ, IC=0.001 <sup>e</sup>	0.6 <sup>g</sup>		0.776	0.992	0.1 <sup>g</sup>		0.848	0.998
COSMO-RS/BP/TZVP <sup>f</sup>					3.2	3.3	0.926	0.983
COSMO-RS/BP/TZVP <sup>f</sup>					0.8 <sup>g</sup>	1.0 <sup>g</sup>	1.060	0.983

<sup>a</sup> This work. <sup>b</sup> Reference 66b. <sup>c</sup> Reference 66c. <sup>d</sup> With the latest experimental  $pK_a$  value for phenol. <sup>e</sup> Reference 59. <sup>f</sup> Reference 62 values for the group of phenols. <sup>g</sup> Based on results predicted by correlations.

From the data in Table 2.9, it follows that achieving both reasonably low mean unsigned error and regression line slope value close to unity at the same time might be a complicated task. In this regard, IEF-PCM, the default solvation method implemented in Gaussian03, combined with the scaled B3LYP/6-311+G\*\* gas-phase data performs rather well in both DMSO and MeCN. This good performance is obviously associated with the quality of underlying gas-phase results. Unfortunately, there is no analysis available about the gas-phase performance of the B3LYP/6-311++G(2df,2p)//B3LYP/6-31+G\* method on compounds studied by Fu et al., and therefore, it is impossible to conclude whether the method might introduce excessive errors for any compounds that could translate into the low slope value in  $pK_a$  correlations. Chipman's SSC(V)PE method demonstrates good performance in terms of mean unsigned error. It is important to note, however, that these MUE values are based on the results predicted by correlations between experimental and calculated  $pK_a$  values and should not be directly compared with other results. The performance of the method depends heavily on the chosen isodensity cutoff value and the

choice of quantum chemical method and basis set. By modifying the isodensity contours it is possible to achieve the slope value of 1; however, the default and recommended cutoff value of 0.001 au resulted in a lower value of slope. Klamt et al.'s COSMO-RS method predicts  $pK_a$  of substituted phenols in MeCN with the mean unsigned error of 0.8  $pK_a$  units. However, this quite good precision is achieved only after applying the results of the correlation between calculated  $\Delta G_{\text{diss}}/RT \ln 10$  and the respective experimental  $pK_a$  values, which were established for the large set of diverse compounds. The raw *ab initio*  $pK_a$  values deviate more substantially from the corresponding experimental values with the mean unsigned error and rms error of 3.2 and 3.3  $pK_a$  units, respectively. The rms error of *ab initio*  $pK_a$  values for the subset of CH acids is much lower, being 0.9–1.1  $pK_a$  units. The authors give the following explanation to the differences in performance: the anionic charge is more delocalized in the case of CH acids as compared to phenols, and therefore, the phenoxide anions exhibit stronger interaction with solvent molecules, which is not fully accounted for by the solvation model.

### 3. Spontaneous Proton Transfer in the Gas Phase

The proton transfer reaction between acid AH and base B can lead directly to the formation of free ions  $A^-$  and  $BH^+$



Assuming the zero activation energy, for the realization of proton transfer the basicity of B must exceed, or at least be comparable to the basicity of the anionic base  $A^-$  (or the acidity of neutral acid AH),  $GB(B) \geq GA(AH)$ . This is the case for the reaction of perchloric acid and potassium or sodium oxide, where the proton transfer (leading to the free separated ions) is energetically favored and should be spontaneous. Indeed, the geometry optimization starting from assumed encounter geometry of acid and base lead to ion-pair complex of the proton transfer reaction products (Figure 3.1).

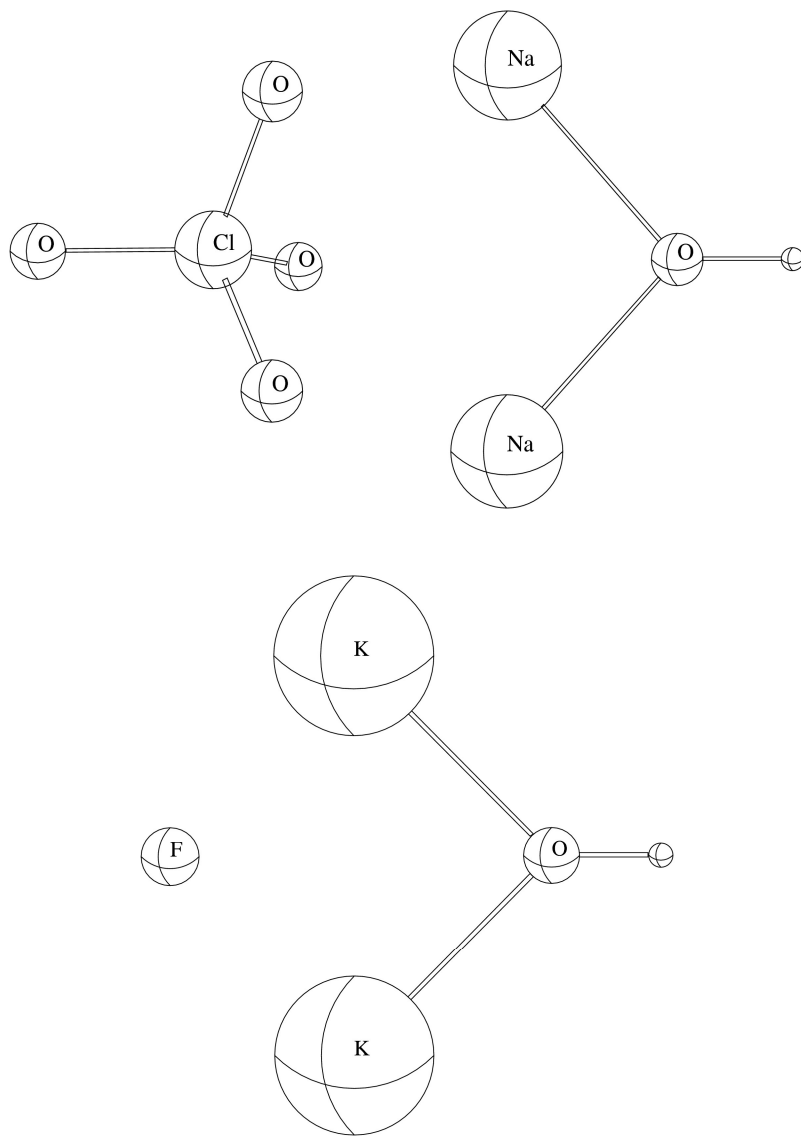
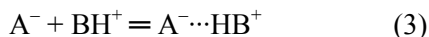


**Figure 3.1.** Typical geometries of proton transfer reaction product complexes between acids and alkali metal oxides

It is important to notice that if the oppositely charged products of the proton-transfer equilibrium (1) might undergo association into the ion-pair as a final product, then the proton transfer reaction should in fact be written as



and its energetic realization will be much more favorable due to rather significant coulombic stabilization through the interaction of its anionic and cationic products



The extent of that electrostatic stabilization can be calculated as a free energy of reaction (3) which is the difference of free energies of processes (2) and (1). The calculated free energies of reactions (1), (2), and (3) are given in Table 3.1 together with calculated gas-phase acidities and basicities.

**Table 3.1.** Gas-Phase Acidities (GA), Basicities (GB), and Free Energies of Reactions (1–3) ( $\Delta G_1$ ,  $\Delta G_2$ ,  $\Delta G_3$ , all in kcal/mol) of Acids HA and Bases B, Calculated at B3LYP/6–311+G\*\* Level

HA	B	GA	GB	$\Delta G_1$	$\Delta G_2$	$\Delta G_3$
HClO <sub>4</sub>	H <sub>2</sub> O	292.5	157.6	134.9	(–1.4) <sup>a</sup>	–136.3
HClO <sub>4</sub>	NH <sub>3</sub>	292.5	195.8	96.7	–4.5 <sup>b</sup>	–103.6
HClO <sub>4</sub>	(H <sub>2</sub> N) <sub>3</sub> P=NH	292.5	241.6	50.9	–27.4	–78.3
HClO <sub>4</sub>	Li <sub>2</sub> O	292.5	278.6	13.9	–101.1	–115.0
HClO <sub>4</sub>	Na <sub>2</sub> O	292.5	309.1	–16.6	–118.5	–101.9
HClO <sub>4</sub>	K <sub>2</sub> O	292.5	322.8	–30.3	–119.3	–89.1
HCl	K <sub>2</sub> O	324.0	322.8	1.2	–102.8	–104.0
HF	K <sub>2</sub> O	361.8	322.8	39.0	–91.1	–130.1

<sup>a</sup> Corresponds to the formation of hydrogen bonded acid-base complex, that is, free energy change of the reaction (4) as no ion-pair complex was found. <sup>b</sup> The formation of hydrogen bonded acid-base complex is preferred by 2.4 kcal/mol.

All studied proton transfer reactions involving alkali metal oxides lead to characteristic ion-pair complexes corresponding to proton attached to the oxide oxygen and alkali metal atoms (bearing considerable positive charge: 0.93–0.97 according to the NBO analysis) electrostatically interacting with anion (Figure 3.1).

The proton transfer from acid to base proceeds without any barrier as evidenced by the geometry optimization leading directly to the product ion pair irrespective to the starting geometry.

Similar results are obtained for the interaction of perchloric acid and HP1 phosphazene (H<sub>2</sub>N)<sub>3</sub>P=NH. There are two possible conformations of the ion pair formed: one with three longer (1.87–2.01 Å) Cl—O<sup>–</sup>⋯H—N contacts and another with two shorter (*ca* 1.74 Å) ones. The first one (with three contacts) is by 1.3 kcal/mol more stable. The remaining two bases, ammonia and water, are much weaker compared to the previously described ones. As a result, proton transfer reactions of perchloric acid with those bases do not irreversibly proceed

to the ion-pair complex. The proton transfer reaction starts with formation of hydrogen bonded encounter complex



which may proceed to the ion-pair complex ( $\text{NH}_3$ ) or may not ( $\text{H}_2\text{O}$ ). The reaction of the perchloric acid with ammonia leads to the hydrogen bonded acid–base complex, which is only by 2.4 kcal/mol more stable than ion-pair complex. It seems that the former is stabilized by two additional N—H $\cdots$ O interactions while the ion-pair complex has only one additional such contact as the proton transfer from O to N is accompanied by the 60 degrees rotation of the ammonia relative to N $\cdots$ O axis (Figure 3.2). The reaction barrier between these two complexes (corresponding to the proton transfer and rotation of ammonia) is very small (*ca* 0.2 kcal/mol) and thus the populations of the conformers are defined only by thermodynamics.

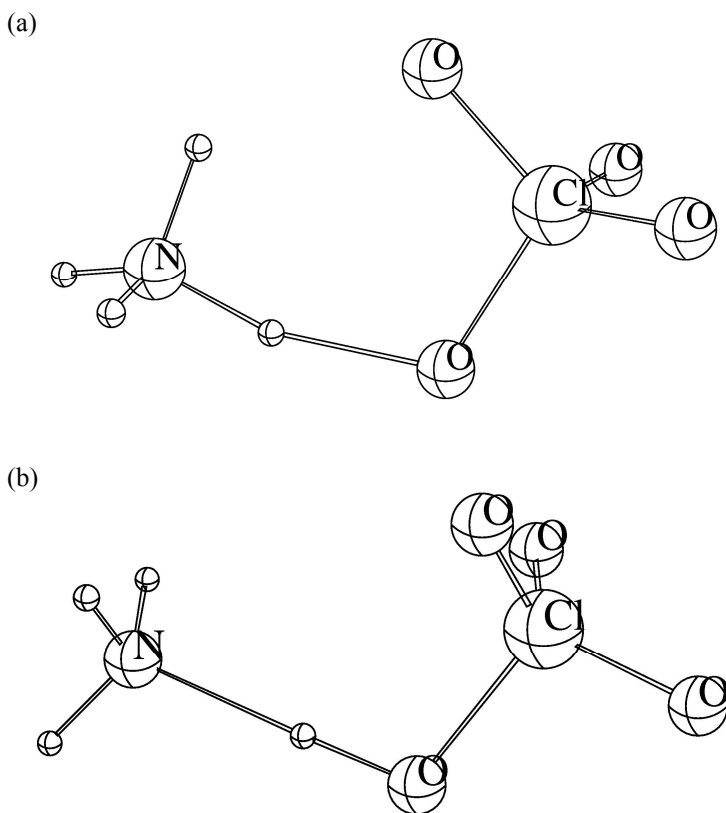


**Figure 3.2.** Geometries of complexes between  $\text{NH}_4^+$  and  $\text{ClO}_4^-$  (a), and  $\text{HClO}_4$  and  $\text{NH}_3$  (b). The second complex is by 2.4 kcal/mol more stable as it has two additional N—H $\cdots$ O contacts compared to one in the first complex

The basicity of water (157.6 kcal/mol) is clearly insufficient for proton transfer and so the reaction is finished by the formation of hydrogen-bonded acid–base complex. Independent of the starting geometry only this complex was obtained with very low hydrogen bond energy ( $\Delta G(4)=1.4$  kcal/mol).

Our results are in qualitative agreement with findings of Alkorta et al.<sup>92</sup> who predicted that for the proton transfer to take place the difference in the proton affinities of base and the acid anion should not exceed 102 kcal/mol. We have shown (the reaction between perchloric acid and ammonia) that splitting up between proton transfer and hydrogen bond formation can occur at the 97 kcal/mol difference between GA and GB.

## CONCLUSIONS

The major results of the present study are summarized below:

1. Our G2 and G3(MP2) calculations indicate that the successive introduction of fluorine atoms into methanol and methanethiol significantly reduces the acidity gap between the representatives of those two series. The G2 calculations predict that the *ca* 25 kcal/mol stronger acidity of CH<sub>3</sub>SH as compared with CH<sub>3</sub>OH is inverted to a -0.1 kcal/mol acidity difference (at 298 K) in the case of the respective trifluoromethyl derivatives. At G3(MP2) level, CF<sub>3</sub>SH is still 0.8 kcal/mol stronger than CF<sub>3</sub>OH on the  $\Delta G_{\text{acid}}$  scale (at 298 K).
2. The energetic effects upon successive fluorination of neutrals, anions, and radicals of the investigated species indicate that hyperconjugation is the main effect in charge for methanols and methanethiols. The same conclusion can be obtained from geometries, especially from the changes of the C–O and C–S bond lengths upon the inclusion of the second and third fluorine atoms. However, the potential energy curves for rotation around the O–H and S–H bonds suggest that the direct electrostatic interactions (i.e., between bond dipoles) should also be taken into account.
3. For FOH and, also, FSH the trends in acidity and basicity upon fluorination of the parent compounds, H<sub>2</sub>O and H<sub>2</sub>S, could be rationalized in terms of field-inductive, polarizability, and (counteracting) lone pair – lone pair repulsion effects.
4. The results of the analysis of the energies, geometries, NBO charges, and topological charge densities together with visualization of the total electron density distributions and selected molecular orbitals indicate that the interaction between DMSO and the anions cannot be characterized in terms of pure electrostatic interaction between the anion and S–O bond dipole. The formation of bidentate hydrogen-bonded complexes was verified, and combined hydrogen bonding and electrostatic charge-dipole interaction should be considered as a more realistic description.
5. The combination of scaled B3LYP/6–311+G\*\* gas-phase acidities with the IEF-PCM method provided reliable absolute  $\text{p}K_{\text{a}}$  values for a diverse set of substituted phenols in the widely used DMSO and MeCN solvents. Our approach binds the scaled gas-phase acidities with optimized solute cavity formation and solvent interactions addressing the charge escape problem. The good predictive power of such an IEF-PCM approach is characterized with a mean unsigned error of 0.6  $\text{p}K_{\text{a}}$  units for DMSO and 0.7  $\text{p}K_{\text{a}}$  units for MeCN. The corresponding correlations between the calculated and experimental  $\text{p}K_{\text{a}}$  values resulted in regression line slopes very close to the expected value of 1.
6. It was shown that spontaneous, unassisted proton transfer can take place in the gas-phase reactions between strong neutral Brønsted acids and bases. The reaction might be barrierless as in case of interactions between extremely strong superacids and superbases (e.g., perchloric acid and alkali

metal oxides or potassium oxide and halogen hydrides) or involve the encounter complex (hydrogen bonded acid–base cluster), which is separated from ion-pair by the transition state. However, it should be kept in mind that such proton transfer reactions do not lead to charge separation (i.e., formation of free protonated base and deprotonated acid) despite the fact that in some studied cases (reaction of  $\text{HClO}_4$  with  $\text{K}_2\text{O}$  or  $\text{Na}_2\text{O}$ ) even that reaction would be energetically favorable. The separation of the ions from the ion-pair is energetically very unfavorable (at least by 80 kcal/mol) and thus the expected product of the proton transfer reaction will be the ion-pair complex.

## REFERENCES

1. Brønsted, J. N. *Rec. Trav. Chim. Pays-Bas* **1923**, *42*, 718.
2. Roberts, J. D.; Webb, R. L.; McElhill, E. A. *J. Am. Chem. Soc.* **1950**, *72*, 408.
3. Burk, P.; Koppel, I. A.; Koppel, I.; Leito, I.; Travnikova, O. *Chem. Phys. Lett.* **2000**, *323*, 482.
4. Tomasi, J.; Mennucci, B.; Cammi, R. *Chem. Rev.* **2005**, *105*, 2999.
5. (a) Kelly, C. P.; Cramer, C. J.; Truhlar, D. G. *J. Phys. Chem. A* **2006**, *110*, 2493. (b) Bryantsev, V. S.; Diallo, M. S.; Goddard, W. A., III. *J. Phys. Chem. B* **2008**, *112*, 9709.
6. (a) Liptak, M. D.; Shields, G. C. *J. Am. Chem. Soc.* **2001**, *123*, 7314. (b) Liptak, M. D.; Gross, K. C.; Seybold, P. G.; Feldgus, S.; Shields, G. C. *J. Am. Chem. Soc.* **2002**, *124*, 6421.
7. Moissan, H. *Le Fluor et ces Composes*; Masson: Paris, 1900.
8. Cady, G. H. *J. Am. Chem. Soc.* **1935**, *57*, 246.
9. Dennis, L. M.; Rochow, E. G. *J. Am. Chem. Soc.* **1932**, *54*, 832.
10. Dennis, L. M.; Rochow, E. G. *J. Am. Chem. Soc.* **1933**, *55*, 2431.
11. Noble, P. N.; Pimentel, G. C. *Spectrochim. Acta, Part A* **1968**, *24*, 797.
12. Appelman, E. H.; Thompson, R. C. *J. Am. Chem. Soc.* **1984**, *106*, 4167.
13. Kim Hyunyong; Pearson, E. F.; Appelman, E. H. *J. Chem. Phys.* **1972**, *56*, 1.
14. Pearson, E. F.; Kim Hyunyong, *J. Chem. Phys.* **1972**, *57*, 4230.
15. Goleb, J. A.; Claassen, H. H.; Studier, M. H.; Appelman, E. H. *Spectrochim. Acta, Part A* **1972**, *28*, 65.
16. Kim Hyunyong; Appelman, E. H. *J. Chem. Phys.* **1982**, *76*, 1664.
17. Christe, K. O. *J. Fluorine Chem.* **1987**, *35*, 621.
18. Appelman, E. H.; Kim Hyunyong. *J. Chem. Phys.* **1972**, *57*, 1972.
19. Appelman, E. H. *Acc. Chem. Res.* **1973**, *6*, 113.
20. Halonen, L.; Ha, T. K. *J. Chem. Phys.* **1988**, *89*, 4885.
21. Thiel, W.; Scuseria, G.; Schaefer, H. F.; Allen, W. D. *J. Chem Phys.* **1988**, *89*, 4965.
22. Pople, J. A.; Curtiss, L. A. *J. Chem. Phys.* **1989**, *90*, 2833.
23. Peterson, K. A.; Woods, R. C. *J. Chem. Phys.* **1990**, *92*, 7412.
24. Koppel, I. A.; Comisarow, M. B. *Org. React.* **1980**, *17*, 495.
25. Koppel, I. A.; Mölder, U. H. *Org. React.* **1981**, *18*, 42.
26. Alcami, M.; Mó, O.; Yáñez, M.; Abboud, J.-L. M.; Elguero, J. *Chem. Phys. Lett.* **1990**, *172*, 471.
27. Taft, R. W.; Koppel, I. A.; Topsom, R. D.; Anvia, F. *J. Am. Chem. Soc.* **1991**, *112*, 2047.
28. Baulch, D. L.; Cox, R. A.; Crutzen, P. J.; Hampson, R. F., Jr.; Ken, J. A.; Troe, Watson, R. T. *J. Phys. Chem. Ref. Data* **1982**, *11*, 327.
29. Thynne, J. C. J.; MacNeil, K. A. G. *J. Mass Spectrom. Ion Phys.* **1970**, *5*, 95.
30. Alekseev, V. I.; Volkov, V. M.; Fedorova, L. I.; Baluev, A. V. *Izv. Akad. Nauk SSSR Ser. Khim.* **1984**, 1302.
31. (a) March, J. *Advanced Organic Chemistry*, 4th ed.; Wiley: New York, 1992; p 266. (b) Ege, S. *Organic Chemistry*, 2nd ed.; D. C. Heath: Lexington; 1989; p 85.
32. Bartmess, J. E.; Scott, J. A.; McIver, R. T., Jr. *J. Am. Chem. Soc.* **1979**, *101*, 6047. Value altered from the reference by Bartmess due to a change in the acidity scale, <http://webbook.nist.gov>.

33. (a) Atkinson, R.; Cox R. A.; Lesclaux, R.; Niki, H.; Zellner, R. *Scientific Assessment of Stratospheric Ozone: 1989*; WMO Report No. 20; 1989; Vol. 2, p 159. (b) Francisco, J. S.; Maricq, M. M. *Acc. Chem. Res.* **1996**, *29*, 391.
34. Huey, L. G.; Dunlea, E. J.; Howard, C. J. *J. Phys. Chem.* **1996**, *100*, 6504.
35. (a) Koppel, I. A.; Taft, R. W.; Anvia, F.; Shi-Zheng Zhu; Li-Quing Hu; Kuang-Sen Sun; DesMarteau, D. D.; Yagupolskii, L. M.; Yagupolskii, Yu. L.; Ignat'ev, N. V.; Kondratenko, N. V.; Volkonskii, A. Yu.; Vlassov, V. M.; Notario, R.; Maria, P.-C. *J. Am. Chem. Soc.* **1994**, *116*, 3047. (b) Koppel, I. A.; Koppel, J.; Pihl, V.; Anvia, F.; Taft, R. W. *J. Am. Chem. Soc.* **1994**, *116*, 8654.
36. Notario, R.; Castaño, O.; Abboud, J. L. M. *Chem. Phys. Lett.* **1996**, *263*, 367.
37. Segovia, M.; Ventura, O. N. *Chem. Phys. Lett.* **1997**, *277*, 490.
38. (a) McMillan, D. F.; Golden D. M. *Annu. Rev. Phys. Chem.* **1982**, *33*, 493. (b) Descamps, B.; Forst, W. *J. Phys. Chem.* **1976**, *80*, 933.
39. Schneider, W. F.; Wallington, T. J. *J. Phys. Chem.* **1993**, *97*, 12783.
40. Marshall, P.; Schwartz, M. J. *J. Phys. Chem. A* **1997**, *101*, 2906.
41. (a) Hoffmann, R.; Radom, L.; Pople, J. A.; Schleyer, P. v. R.; Hehre, W.; Salem, L. *J. Am. Chem. Soc.* **1972**, *95*, 6221. (b) David, S.; Eisenstein, O.; Hehre, W.; Salem, L.; Hoffmann, R. *J. Am. Chem. Soc.* **1973**, *95*, 3806.
42. Schleyer, P. v. R.; Kos, A. J. *Tetrahedron* **1983**, *39*, 1141.
43. Schneider, W. F.; Nance, B. I.; Wallington, T. J. *J. Am. Chem. Soc.* **1995**, *117*, 478.
44. Magnera, T. F.; Caldwell, G.; Sunner, J.; Ikuta, S.; Kebarle, P. *J. Am. Chem. Soc.* **1984**, *106*, 6140.
45. Kebarle, P.; Caldwell, G.; Magnera, T.; Sunner, J. *Pure Appl. Chem.* **1985**, *57*, 339.
46. Koppel, I. A.; Mölder, U. H. *Org. React.* **1983**, *20*, 3.
47. Koppel, I. A. *Org. React.* **1987**, *24*, 263.
48. Sieck, L. W. *J. Phys. Chem.* **1985**, *89*, 5552.
49. Trummel, A.; Rummel, A.; Koppel, I. A.; Lippmaa, E. Formation of DMSO – Anion Clusters: Theoretical and Experimental Approach. *Presented at the Second World Congress of Theoretical Organic Chemists*, University of Toronto, Toronto, July 8–14, 1990; CP-20.
50. Brown, I. D. *J. Sol. Chem.* **1987**, *16*, 205.
51. Abboud, J.-L.; Notario, R.; Botella, V. In *Theoretical Computational Chemistry*, Politzer, P., Murray, J. S., Eds., Elsevier, Amsterdam, 1994, Vol. 1, pp 135–182.
52. Murłowska, K.; Sadlej-Sosnowska, N. *J. Phys. Chem. A* **2005**, *109*, 5590.
53. da Silva, G.; Kennedy, E. M.; Długogorski, B. Z. *J. Phys. Chem. A* **2006**, *110*, 11371.
54. Kallies, B.; Mitzner, R. *J. Phys. Chem. B* **1997**, *101*, 2959.
55. Takano, Y.; Houk, K. N. *J. Chem. Theory Comput.* **2005**, *1*, 70.
56. Gutowski, K. E.; Dixon, D. A. *J. Phys. Chem. A* **2006**, *110*, 12044.
57. Pliego, J. R., Jr.; Riveros, J. M. *J. Phys. Chem. A* **2002**, *106*, 7434.
58. Klamt, A.; Eckert, F.; Diedenhofen, M.; Beck, M. E. *J. Phys. Chem. A* **2003**, *107*, 9380.
59. Chipman, D. M. *J. Phys. Chem. A* **2002**, *106*, 7413.
60. Almerindo, G. I.; Tondo, D. W.; Pliego, J. R., Jr. *J. Phys. Chem. A* **2004**, *108*, 166.
61. Qi, X.-J.; Liu, L.; Fu, Y.; Guo, Q.-X. *Organometallics* **2006**, *25*, 5879.
62. Eckert, F.; Leito, I.; Kaljurand, I.; Kütt, A.; Klamt, A.; Diedenhofen, M. *J. Comput. Chem.* **2008**, *30*, 799.

63. Kovačević, B.; Maksić, Z. B. *Org. Lett.* **2001**, *3*, 1523.
64. Magill, A. M.; Cavell, K. J.; Yates, B. F. *J. Am. Chem. Soc.* **2004**, *126*, 8717.
65. Foresman, J. B.; Keith, T. A.; Wiberg, K. B.; Snoonian, J.; Frisch, M. J. *J. Phys. Chem.* **1996**, *100*, 16098.
66. (a) Fu, Y.; Liu, L.; Li, R.-Q.; Liu, R.; Guo, Q.-X. *J. Am. Chem. Soc.* **2004**, *126*, 814. (b) Fu, Y.; Liu, L.; Wang, Y.-M.; Li, J.-N.; Yu, T.-Q.; Guo, Q.-X. *J. Phys. Chem. A* **2006**, *110*, 5874. (c) Fu, Y.; Liu, L.; Yu, H.-Z.; Wang, Y.-M.; Guo, Q.-X. *J. Am. Chem. Soc.* **2005**, *127*, 7227.
67. (a) Cancès, E.; Mennucci, B.; Tomasi, J. *J. Chem. Phys.* **1997**, *107*, 3032. (b) Mennucci, B.; Tomasi, J. *J. Chem. Phys.* **1997**, *106*, 5151. (c) Mennucci, B.; Cancès, E.; Tomasi, J. *J. Phys. Chem. B* **1997**, *101*, 10506. (d) Tomasi, J.; Mennucci, B.; Cancès, E. *J. Mol. Struct.: THEOCHEM* **1999**, *464*, 211.
68. Bartmess, J. NIST Chemistry WebBook, NIST Standard Reference Database Number 69; National Institute of Standards and Technology: Gaithersburg, MD, 2005. <http://webbook.nist.gov>.
69. Koppel, I. A.; Burk, P.; Koppel, I.; Leito, I.; Sonoda, T.; Mishima, M. *J. Am. Chem. Soc.* **2000**, *122*, 5114.
70. Koppel, I. A.; Burk, P.; Koppel, I.; Leito, I. *J. Am. Chem. Soc.* **2002**, *124*, 5594.
71. Maksić, Z. B.; Vianello, R. *Pure Appl. Chem.* **2007**, *79*, 1003.
72. Krossing, I.; Raabe, I. *Angew. Chem. Int. Ed.* **2004**, *43*, 2066.
73. Stoyanov, E. S.; Kim, K.-C.; Reed, C. A. *J. Am. Chem. Soc.* **2006**, *128*, 8500.
74. Reed, C. A. *Chem. Comm.* **2005**, 1669.
75. Hunter, E.; Lias, S. NIST Chemistry WebBook, NIST Standard Reference Database Number 69; National Institute of Standards and Technology: Gaithersburg, MD, 2005. <http://webbook.nist.gov>.
76. Kaljurand, I.; Koppel, I. A.; Kütt, A.; Rõõm, E.-I.; Rodima, T.; Koppel, I.; Mishima, M.; Leito, I. *J. Phys. Chem. A* **2007**, *111*, 1245.
77. Butman, M. F.; Kudin, L. S.; Krasnov, K. S. *Russ. J. Inorg. Chem. (Transl. Zh. Neorg. Khim.)* **1984**, *29*, 2150.
78. Burk, P.; Koppel, I. A. *Int. J. Quant. Chem.* **1994**, *51*, 313.
79. Burk, P.; Sillar, K.; Koppel, I. A. *J. Mol. Struct.: THEOCHEM* **2001**, *543*, 223.
80. Burk, P.; Tamp, S. *J. Mol. Struct.: THEOCHEM* **2003**, *638*, 119.
81. Raab, V.; Gauchenova, E.; Merkoulov, A.; Harms, K.; Sundermeyer, J.; Kovačević, B.; Maksić, Z. B. *J. Am. Chem. Soc.* **2005**, *127*, 15738.
82. Kovačević, B.; Maksić, Z. B. *Chem. Comm.* **2006**, 1524.
83. Koppel, I. A.; Schwesinger, R.; Breuer, T.; Burk, P.; Herodes, K.; Koppel, I.; Leito, I.; Mishima, M. *J. Phys. Chem. A* **2001**, *105*, 9575.
84. Kolomeitsev, A. A.; Koppel, I. A.; Rodima, T.; Barten, J.; Lork, E.; Rösenthaller, G.-V.; Kaljurand, I.; Kütt, A.; Koppel, I.; Mäemets, V.; Leito, I. *J. Am. Chem. Soc.* **2005**, *127*, 17656.
85. Catalan, J. *J. Org. Chem.* **1999**, *64*, 1908.
86. Koppel, I. A.; Anvia, F.; Taft, R. W. *Presented at the Second World Congress of Theoretical Organic Chemists*, University of Toronto, Toronto, July 8–14, 1990; B1-O7.
87. Koppel, I. *J. Chim. Phys. Phys.-Chim. Biol.* **1992**, *89*, 1545.
88. Catalan, J.; Palomar, J. *Chem. Phys. Lett.* **1998**, *293*, 511.
89. Mó, O.; Yáñez, M.; Gonzales, L.; Elguero, J. *ChemPhysChem* **2001**, *2*, 465.
90. Benco, L.; Demuth, T.; Hafner, J.; Hutschka, F. *Chem. Phys. Lett.* **2000**, *330*, 457.
91. Simons, S.; Sodupe, M.; Bertran, J. *Theor. Chem. Acc.* **2004**, *111*, 217.

92. Alkorta, I.; Rozas, I.; M $\acute{o}$ , O.; Y $\acute{a}$ ñez, M.; Elguero, J. *J. Phys. Chem. A* **2001**, *105*, 7481.
93. Huh, Y. D.; Cross, R. J.; Saunders, M. *J. Am. Chem. Soc.* **1990**, *112*, 3774.
94. Hehre, W. J.; Radom, L.; Schleyer, P. v. R.; Pople, J. A. *Ab Initio Molecular Orbital Theory*; Wiley: New York, 1986.
95. Frisch, M. J.; Trucks, G. W.; Schlegel, H. B.; Scuseria, G. E.; Robb, M. A.; Cheeseman, J. R.; Montgomery, J. A., Jr.; Vreven, T.; Kudin, K. N.; Burant, J. C.; Millam, J. M.; Iyengar, S. S.; Tomasi, J.; Barone, V.; Mennucci, B.; Cossi, M.; Scalmani, G.; Rega, N.; Petersson, G. A.; Nakatsuji, H.; Hada, M.; Ehara, M.; Toyota, K.; Fukuda, R.; Hasegawa, J.; Ishida, M.; Nakajima, T.; Honda, Y.; Kitao, O.; Nakai, H.; Klene, M.; Li, X.; Knox, J. E.; Hratchian, H. P.; Cross, J. B.; Bakken, V.; Adamo, C.; Jaramillo, J.; Gomperts, R.; Stratmann, R. E.; Yazyev, O.; Austin, A. J.; Cammi, R.; Pomelli, C.; Ochterski, J. W.; Ayala, P. Y.; Morokuma, K.; Voth, G. A.; Salvador, P.; Dannenberg, J. J.; Zakrzewski, V. G.; Dapprich, S.; Daniels, A. D.; Strain, M. C.; Farkas, O.; Malick, D. K.; Rabuck, A. D.; Raghavachari, K.; Foresman, J. B.; Ortiz, J. V.; Cui, Q.; Baboul, A. G.; Clifford, S.; Cioslowski, J.; Stefanov, B. B.; Liu, G.; Liashenko, A.; Piskorz, P.; Komaromi, I.; Martin, R. L.; Fox, D. J.; Keith, T.; Al-Laham, M. A.; Peng, C. Y.; Nanayakkara, A.; Challacombe, M.; Gill, P. M. W.; Johnson, B.; Chen, W.; Wong, M. W.; Gonzalez, C.; Pople, J. A. *Gaussian 03*, revision B.04; Gaussian, Inc.: Wallingford, CT, 2004.
96. Pople, J. A.; Head-Gordon, M.; Fox, D. J.; Raghavachari, K.; Curtiss, L. A. *J. Chem. Phys.* **1989**, *90*, 5622.
97. Curtiss, L. A.; Raghavachari, K.; Trucks, G. W.; Pople, J. A. *J. Chem. Phys.* **1991**, *94*, 7221.
98. Becke, A. D. *J. Chem. Phys.* **1993**, *98*, 5648.
99. Vosko, S. H.; Wilk, L.; Nusair, M. *Can. J. Phys.* **1980**, *58*, 1200.
100. Lee, C.; Yang, W.; Parr, R. G. *Phys. Rev. B* **1988**, *37*, 785.
101. Mielich, B.; Savin, A.; Stoll, H.; Preuss, H. *Chem. Phys. Lett.* **1989**, *157*, 200.
102. Kütt, A.; Movchun, V.; Rodima, T.; Dansauer, T.; Rusanov, E. B.; Leito, I.; Kaljurand, I.; Koppel, J.; Pihl, V.; Koppel, I.; Ovsjannikov, G.; Toom, L.; Mishima, M.; Medebielle, M.; Lork, E.; Röschenthaler, G.-V.; Koppel, I. A.; Kolomeitsev, A. A. *J. Org. Chem.* **2008**, *73*, 2607.
103. Tissandier, M. D.; Cowen, K. A.; Feng, W. Y.; Gundlach, E.; Cohen, M. H.; Earhart, A. D.; Coe, J. V.; Tuttle, T. R. *J. Phys. Chem. A* **1998**, *102*, 7787.
104. Marcus, Y. *Pure Appl. Chem.* **1983**, *55*, 977.
105. Bader, R. F. W. *Atoms in Molecules: A Quantum Theory*, Oxford University Press, Oxford, 1989.
106. Biegler-König, F. W.; Bader, R. F. W.; Ting-Hua, T. *J. Comput. Chem.* **1982**, *3*, 317.
107. (a) Carpenter, J. E.; Weinhold, F. *J. Mol. Struct.: THEOCHEM* **1988**, *169*, 41. (b) Carpenter, J. E. PhD thesis, University of Wisconsin, Madison, WI, 1987. (c) Foster, J. P.; Weinhold, F. *J. Am. Chem. Soc.* **1980**, *102*, 7211. (d) Reed, A. E.; Weinhold, F. *J. Chem. Phys.* **1983**, *78*, 4066. (e) Reed, A. E.; Weinstock, R. B.; Weinhold, F. *J. Chem. Phys.* **1985**, *83*, 735. (f) Reed, A. E.; Curtiss, L. A.; Weinhold, F. *Chem. Rev.* **1988**, *88*, 899. (g) Weinhold, F.; Carpenter, J. E. *Plenum* **1988**, 227.
108. *Molekel, Revision 3.04*, Flükiger, P. F.; Portmann, S., University of Geneva, CSCS/SCSC-ETHZ, Switzerland.

109. (a) Wiberg, K. B.; Laidig, K. E. *J. Am. Chem. Soc.* **1988**, *110*, 1872. (b) Wang, X.; Houk, K. N. *J. Am. Chem. Soc.* **1988**, *110*, 1870.
110. Brockway, L. O. *J. Phys. Chem.* **1937**, *41*, 185.
111. (a) Reed, A. E.; Schleyer, P. v. R. *J. Am. Chem. Soc.* **1987**, *109*, 7362. (b) Salzner, U.; Schleyer, P. v. R. *Chem. Phys. Lett.* **1992**, *190*, 401.
112. Wiberg, K. B.; Rablen, P. R. *J. Am. Chem. Soc.* **1993**, *115*, 614.
113. Koppel, I. A.; Burk, P.; Koppel, I.; Leito, I. Unpublished results.
114. Schulz, P. A.; Mead, R. D.; Jones, P. L.; Lineberger, W. C. *J. Chem. Phys.* **1982**, *77*, 1153.
115. Gilles, M. K.; Polak, M. L.; Lineberger, W. C. *J. Chem. Phys.* **1992**, *96*, 8012.
116. Molina, M. T.; Bouab, W.; Essefar, M.; Herreros, M.; Notario, R.; Abboud, J.-L. M.; M $\acute{o}$ , O.; Y $\acute{a}$ ñez, M. *J. Org. Chem.* **1996**, *61*, 5485.
117. Lias, S. G.; Bartmess, J. E.; Liebman, J. F.; Holmes, J. L.; Levin, R. D.; Mallard, W. G. *J. Phys. Chem. Ref. Data* **1988**, *17* (Suppl. 1).
118. Koppel, I. A.; Molder, U. H. *Org. React.* **1983**, *20*, 3.
119. Hansch, C.; Leo, A.; Taft, R. W. *Chem. Rev.* **1991**, *91*, 165.
120. Arshadi, M.; Kebarle, P. *J. Phys. Chem.* **1970**, *74*, 1483.
121. Payzant, J. D.; Yamdagni, R.; Kebarle, P. *Can. J. Chem.* **1971**, *49*, 3308.
122. Yamdagni, R.; Kebarle, P. *J. Am. Chem. Soc.* **1971**, *93*, 7139.
123. Bordwell, F. G. *Acc. Chem. Res.* **1988**, *21*, 456.
124. Kaljurand, I.  $pK_a$  Data of Acids and Bases; University of Tartu: Tartu, Estonia, 2000. <http://tera.chem.ut.ee/~manna/pkadata.xls>.
125. Reich, H. J. Bordwell  $pK_a$  Table (Acidity in DMSO); University of Wisconsin: Madison, WI, 2007. <http://www.chem.wisc.edu/areas/reich/pkatable/>.
126. Izutsu, K. *Acid-Base Dissociation Constants in Dipolar Aprotic Solvents*; IUPAC Chemical Data Series No. 35; Blackwell Scientific: Oxford, 1990.
127. Chantooni, M. K.; Kolthoff, I. M. *J. Phys. Chem.* **1976**, *80*, 1306.
128. Vlasov, V. M.; Sheremet, O. P. *Izv. Sib. Otd. Akad. Nauk SSSR, Ser. Khim. Nauk* **1982**, 114.
129. Westphal, E.; Pliego, J. R. *J. Chem. Phys.* **2005**, *123*, 074508.
130. Kelly, C. P.; Cramer, C. J.; Truhlar, D. G. *J. Phys. Chem. B* **2007**, *111*, 408.
131. (a) K $\ddot{u}$ tt, A.; Leito, I.; Kaljurand, I.; Soov $\ddot{a}$ li, L.; Vlasov, V. M.; Yagupolskii, L. M.; Koppel, I. A. *J. Org. Chem.* **2006**, *71*, 2829. (b) Leito, I.; K $\ddot{u}$ tt, A.; Kaljurand, I.; R $\ddot{o}$ dm, E.-I.; Rodima, T.; Koppel, I. A. *Presented at the 233rd American Chemical Society National Meeting*; Chicago, IL, March 25–27, 2007; INOR 1036.

## SUMMARY IN ESTONIAN

### Struktuuri- ja solvendiefektide mõju arvutuslik uurimine Brønstedi hapete happelisusele

Käesolevas töös uuriti kõrgetasemeliste *ab initio* meetoditega oluliste struktuursete faktorite (suure elektronegatiivsusega F aatomi olemasolu ning kõrvuti-asetsevate hapniku ja fluori aatomite vabade elektronpaaride vaheline interaktsioon) mõju FOH molekuli happelisusele ja aluselisusele. G2 meetodit kasutades arvutati  $\text{CH}_{3-n}\text{F}_n\text{OH}$  ja  $\text{CH}_{3-n}\text{F}_n\text{SH}$  ( $n = 0-3$ ) seeriate happelisused ning selgitati välja võtmefaktorid, mis avaldavad mõju nii nende OH ja SH hapete kui ka nende heterolüütilise ja homolüütilise dissotsiatsiooni produktide geomeetria- ja energetikale.

Teiseks uurimisteenaks oli DMSO ja anioonide vahelise komplekseerumise iseloomu väljaselgitamine ning IEF-PCM meetodi ennustusvõime hindamine asendatud fenoolide  $pK_a$  väärtuste arvutamisel dimetüülsulfoksiidis ja atsetonitriilis.

Samuti uuriti käesolevas töös tugeva aluse ( $\text{K}_2\text{O}$ ) interaktsiooni erineva tugevusega hapetega ( $\text{HClO}_4$ ,  $\text{HCl}$  ja  $\text{HF}$ ) ning tugeva happe ( $\text{HClO}_4$ ) interaktsiooni alustega alates  $\text{K}_2\text{O}$ -st kuni  $\text{H}_2\text{O}$ -ni, et selgitada välja partneritevahelise prootoniülekanne iseloom ja ulatus.

Uurimistöö olulisemad tulemused on esitatud alljärgnevas loetelus:

1. Meie G2 and G3(MP2) arvutused näitavad, et fluori aatomite järjestikune sisseviimine metanooli ja metaantiooli vähendab oluliselt happelisuse vahet nende kahe seeria esindajate vahel. G2 arvutused ennustavad, et  $\text{CH}_3\text{SH}$  ca 25 kcal/mol tugevam happelisus võrrelduna  $\text{CH}_3\text{OH}$ -ga pöörduv  $-0,1$  kcal/mol happelisuse erinevuseks (temperatuuril 298 K) vastavate trifluorometüül derivaatide korral. G3(MP2) tasemel on  $\text{CF}_3\text{SH}$  ikka 0,8 kcal/mol tugevam kui  $\text{CF}_3\text{OH}$   $\Delta G_{\text{acid}}$  skaalas (temperatuuril 298 K).
2. Energeetilised efektid uuritud ühendite neutraalsete vormide, anioonide ja radikaalide järjestikusel fluoreerimisel näitavad, et hüperkonjugatsioon on metanoolide ja metaantioolide jaoks peamine mõjuv faktor. Sama järelduseni võib jõuda ka geomeetriaest, eriti C–O ja C–S sidemepikkuste muutumisest teise ja kolmanda fluori aatomi lisamisel. Siiski nähtub potentsiaalse energia kõveratest, mis saadakse struktuuri rotatsioonil O–H ja S–H sidemete suhtes, et arvestada tuleks ka otseseid elektrostaatilisi (s.t. sideme dipoolide vahelisi) interaktsioone.
3. FOH ning samuti FSH korral saab happelisuse ja aluselisuse muutumist lähteühendite  $\text{H}_2\text{O}$  ja  $\text{H}_2\text{S}$  fluoreerimisel selgitada induktsiooni, polariseeritavuse ja (vastutoimiva) vabade elektronpaaride omavahelise tõukumise efektidega.
4. Energiate, geomeetria, NBO laengute ja topoloogiliste laengutiheduste analüüsi tulemused koos summaarse elektrontiheduse jaotuse ja valitud

- molekulorbitaalide visualiseerimisega näitavad, et interaktsiooni DMSO ja anioonide vahel ei saa iseloomustada puhta elektrostaatilisest interaktsiooniga aniooni ja S–O sideme dipooli vahel. Tõendati bidentaatsete vesiniksidemete komplekside tekkimine ning pakuti välja vesiniksidemete moodustumise ja elektrostaatilisest laeng–dipool vastasmõju kombinatsioon kui arvestatav mõjufaktor DMSO ja anioonide kompleksimoodustamise kirjeldamisel.
5. Skaleeritud B3LYP/6–311+G\*\* gaasifaasi happelisuste kombineerimine IEF-PCM meetodiga andis usaldusväärseid absoluutse  $pK_a$  väärtusi mitmesuguste asendatud fenoolide korral laialdaselt kasutatavates DMSO ja MeCN solventides. Meie lähenemine seob skaleeritud gaasifaasi happelisused optimeeritud soluudi õõnsuse moodustamisega ja solvendi interaktsioonidega, mis arvestavad ja kompenseerivad laengu võimalikku leket. Sellise IEF-PCM lähenemise head ennustusvõimet iseloomustab keskmine absoluutne viga 0,6  $pK_a$  ühikut DMSO korral ja 0,7  $pK_a$  ühikut MeCN korral. Vastavatest korrelatsioonidest arvatud ja eksperimentaalsete  $pK_a$  väärtuste vahel saadi regressioonisirge tõusudeks oodatavale väärtusele 1 väga lähedased väärtused.
  6. Näidati, et spontaanne iseeneslik prootoni üleminek võib toimuda gaasifaasi reaktsioonides tugevate neutraalsete Brønsted'i hapete ja aluste vahel. Reaktsioon võib olla barjäärivaba nagu äärmiselt tugevate superhapete ja superaluste (näiteks perkloorhape ja leelismetallioksiidide või kaaliumoksiidi ja halogeenhüdriidide) vaheliste interaktsioonide korral või toimuda ülekohtumiskompleksi (vesiniksidemete hape–alus klaster), mis on eraldatud ioonpaarist aktiveeritud vahekompleksiga. Siiski tuleb silmas pidada, et sellised prootoni ülekandereaktsioonid ei vii laengute eraldumiseni (s.t. vaba protoneeritud aluse ja deprotoneeritud happe moodustumiseni) vaatamata faktile, et mõnedel vaadeldud juhtudel ( $\text{HClO}_4$  reaktsioon  $\text{K}_2\text{O}$  või  $\text{Na}_2\text{O}$ -ga) oleks isegi selline reaktsioon energeetiliselt soodustatud. Ioonide eraldumine ioonpaarist on üldiselt energeetiliselt väga ebasoodne (vähemalt 80 kcal/mol ulatuses) ning seega oleks prootoni ülekandereaktsiooni oodatavaks produktiks ioonpaarkompleks.

## **ACKNOWLEDGEMENTS**

The completion of the present study would have been hardly imaginable without valuable input and continuous support from many people during all these years.

First, I would like to express my sincere gratitude to my doctoral advisors Ilmar Koppel, Peeter Burk, and Endel Lippmaa for their professional guidance, inspiration, and encouragement.

I am also very grateful to all my former scientific supervisors during the studies at University of Tartu, in chronological order, Natalia Palm, Mati Karelson, Viktor Palm, and Viljar Pihl for introducing and teaching various aspects of the research work in chemical sciences.

I am also thankful to my colleagues at the Institute of Chemical Physics and Biophysics for sharing creative scientific environment and nice atmosphere.

Finally, I would like to thank Alar Rummel for countless fruitful discussions and technical advice.

The last but not least, I highly appreciate enormous amount of support, care, inspiration, and understanding I received from my parents and from Katrin, Mikk, and Ann.



## **PUBLICATIONS**

# CURRICULUM VITAE

## Aleksander Trummal

Born: November 19, 1963, Tallinn, Estonia  
Address: National Institute of Chemical Physics and Biophysics  
10 Rävåla Blvd., 10143 Tallinn, Estonia  
Phone: +372 660 5150  
E-mail: aleksander.trummal@kbfi.ee  
Citizenship: Estonian  
Marital status: Married, two children

## Education

1980–1985 Student, Department of Chemistry, University of Tartu  
1985 BSc (Organic Chemistry), *cum laude*  
1986–1988 Graduate Student, Academy of Sciences, NICPB, Physical Chemistry  
2000 MSc (Physical and Analytical Chemistry), *cum laude*  
2000–2005 PhD Student, Institute of Chemical Physics, University of Tartu, Physical and Analytical Chemistry, Supervisors Prof. Ilmar A. Koppel and Prof. Peeter Burk

## Professional experience

1985–1985 NICPB, Laboratory of Chemical Physics, Engineer  
1986–1996 NICPB, Laboratory of Chemical Physics, Junior Researcher  
1996–present NICPB, Laboratory of Chemical Physics, Researcher

## Major publications

1. Trummal, A.; Rummel, A.; Lippmaa, E.; Burk, P.; Koppel, I. A. IEF-PCM Calculations of Absolute  $pK_a$  for Substituted Phenols in Dimethyl Sulfoxide and Acetonitrile Solutions. *J. Phys. Chem. A* **2009**, *113*, 6206–6212.
2. Burk, P.; Koppel, I.; Trummal, A.; Koppel, I. A. Feasibility of the spontaneous gas-phase proton transfer equilibria between neutral Brønsted acids and Brønsted bases. *J. Phys. Org. Chem.* **2008**, *21*, 571–574.
3. Anelli, G.; Lippmaa, E.; Rummel, A.; Trummal, A. et al. The TOTEM Experiment at the CERN Large Hadron Collider. *Journal of Instrumentation* **2008**, *3*, 1–107.

4. Lippmaa, E.; Maremäe, E.; Rummel, A.; Trummal, A. Tantalum, niobium and thorium cake production at the Sillamäe oil shale processing plant. *Oil Shale* **2006**, *23*, 281–285.
5. Lippmaa, E.; Maremäe, E.; Trummal, A.; Rummel, A.; Lippmaa, J. Enriched uranium technology at the Sillamäe oil shale processing plant. *Oil Shale* **2006**, *23*, 275–280.
6. Burk, P.; Koppel, I. A.; Rummel, A.; Trummal, A. Can O-H Acid be More Acidic Than Its S-H Analog? A G2 Study of Fluoromethanols and Fluoromethanethiols. *J. Phys. Chem. A* **2000**, *104*, 1602–1607.
7. Burk, P.; Mölder, U.; Koppel, I. A.; Rummel, A.; Trummal, A. Theoretical Study of Dimethyl Sulfoxide – Anion Clusters. *J. Phys. Chem.* **1996**, *100*, 16137–16140.
8. Burk, P.; Koppel, I. A.; Rummel, A.; Trummal, A. Theoretical Calculation of Intrinsic Acidity and Basicity of FOH. *J. Phys. Chem.* **1995**, *99*, 1432–1435.

### Conferences and meetings

1. The 233rd American Chemical Society National Meeting; Chicago, IL, USA: March 25–29, 2007. Presented poster: Burk, P.; Koppel, I. A.; Koppel, I.; Trummal, A. Feasibility of the Spontaneous Gas-Phase Proton Transfer equilibria Between Neutral Brønsted Acids and Bases. 2007. INOR1037.
2. The 233rd American Chemical Society National Meeting; Chicago, IL, USA: March 25–29, 2007. Presented poster: Koppel, I. A.; Leito, I.; Koppel, I.; Lipping, L.; Trummal, A.; Burk, P. Superacidity and Superbasicity of Neutral Brønsted Acids and Bases: The Limits of Growth. 2007. INOR571.
3. European Conference on Solid State Nuclear Magnetic Resonance, New Concepts and Applications, Chamonix-Mont Blanc, France, September 11–15, 2005. Presented poster: Lippmaa, E.; Sarv, P.; Rummel, A.; Trummal, A. High Temperature 1H MAS-NMR and Combined MOPAC 2002/Gaussian 03 Study of the Lattice-Promoted Proton Transfers in an Active Site of Ferrierite and in other Zeolite Catalysts. 2005. P59.
4. Second World Congress of the Theoretical Organic Chemists, Toronto, Canada, July 8–14, 1990. Presented poster: Trummal, A.; Rummel, A.; Koppel, I. A.; Lippmaa, E. Formation of DMSO – Anion Clusters: Theoretical and Experimental Approach. 1990. CP-20.

# CURRICULUM VITAE

## Aleksander Trummal

Sünniaeg ja -koht: 19. november, 1963. aasta, Tallinn, Eesti  
Aadress: Keemilise ja Bioloogilise Füüsika Instituut  
Rävala pst. 10, 10143 Tallinn, Eesti  
Telefon: +372 660 5150  
E-post: aleksander.trummal@kbfi.ee  
Kodakondsus: Eesti  
Perekonnaseis: Abielus, kaks last

## Haridus

1980–1985 Tartu Ülikool, Keemiaosakond, üliõpilane  
1985 BSc orgaanilises keemias, *cum laude*  
1986–1988 Teaduste Akadeemia KBFI, aspirantuur, füüsikaline keemia  
2000 MSc füüsikalises ja analüütilises keemias, *cum laude*  
2000–2005 Tartu Ülikool, Keemilise Füüsika Instituut, doktorantuur, füüsikaline ja analüütiline keemia, juhendajad Prof. Ilmar A. Koppel and Prof. Peeter Burk

## Teenistuskäik

1985–1985 KBFI, keemilise füüsika labor, insener  
1986–1996 KBFI, keemilise füüsika labor, nooremteadur  
1996–praeguseni KBFI, keemilise füüsika labor, teadur

## Tähtsamad teaduspublikatsioonid

1. Trummal, A.; Rummel, A.; Lippmaa, E.; Burk, P.; Koppel, I. A. IEF-PCM Calculations of Absolute  $pK_a$  for Substituted Phenols in Dimethyl Sulfoxide and Acetonitrile Solutions. *J. Phys. Chem. A* **2009**, *113*, 6206–6212.
2. Burk, P.; Koppel, I.; Trummal, A.; Koppel, I. A. Feasibility of the spontaneous gas-phase proton transfer equilibria between neutral Brønsted acids and Brønsted bases. *J. Phys. Org. Chem.* **2008**, *21*, 571–574.
3. Anelli, G.; Lippmaa, E.; Rummel, A.; Trummal, A. et al. The TOTEM Experiment at the CERN Large Hadron Collider. *Journal of Instrumentation* **2008**, *3*, 1–107.

4. Lippmaa, E.; Maremäe, E.; Rummel, A.; Trummal, A. Tantalum, niobium and thorium cake production at the Sillamäe oil shale processing plant. *Oil Shale* **2006**, *23*, 281–285.
5. Lippmaa, E.; Maremäe, E.; Trummal, A.; Rummel, A.; Lippmaa, J. Enriched uranium technology at the Sillamäe oil shale processing plant. *Oil Shale* **2006**, *23*, 275–280.
6. Burk, P.; Koppel, I. A.; Rummel, A.; Trummal, A. Can O-H Acid be More Acidic Than Its S-H Analog? A G2 Study of Fluoromethanols and Fluoromethanethiols. *J. Phys. Chem. A* **2000**, *104*, 1602–1607.
7. Burk, P.; Mölder, U.; Koppel, I. A.; Rummel, A.; Trummal, A. Theoretical Study of Dimethyl Sulfoxide – Anion Clusters. *J. Phys. Chem.* **1996**, *100*, 16137–16140.
8. Burk, P.; Koppel, I. A.; Rummel, A.; Trummal, A. Theoretical Calculation of Intrinsic Acidity and Basicity of FOH. *J. Phys. Chem.* **1995**, *99*, 1432–1435.

### **Osalemine konverentsidel**

1. The 233rd American Chemical Society National Meeting; Chicago, IL, USA: March 25–29, 2007. Esitatud poster: Burk, P.; Koppel, I. A.; Koppel, I.; Trummal, A. Feasibility of the Spontaneous Gas-Phase Proton Transfer equilibria Between Neutral Brönsted Acids and Bases. 2007. INOR1037.
2. The 233rd American Chemical Society National Meeting; Chicago, IL, USA: March 25–29, 2007. Esitatud poster: Koppel, I. A.; Leito, I.; Koppel, I.; Lipping, L.; Trummal, A.; Burk, P. Superacidity and Superbasicity of Neutral Brönsted Acids and Bases: The Limits of Growth. 2007. INOR571.
3. European Conference on Solid State Nuclear Magnetic Resonance, New Concepts and Applications, Chamonix-Mont Blanc, France, September 11–15, 2005. Esitatud poster: Lippmaa, E.; Sarv, P.; Rummel, A.; Trummal, A. High Temperature 1H MAS-NMR and Combined MOPAC 2002/Gaussian 03 Study of the Lattice-Promoted Proton Transfers in an Active Site of Ferrierite and in other Zeolite Catalysts. 2005. P59.
4. Second World Congress of the Theoretical Organic Chemists, Toronto, Canada, July 8–14, 1990. Esitatud poster: Trummal, A.; Rummel, A.; Koppel, I. A.; Lippmaa, E. Formation of DMSO – Anion Clusters: Theoretical and Experimental Approach. 1990. CP-20.

## DISSERTATIONES CHIMICAE UNIVERSITATIS TARTUENSIS

1. **Toomas Tamm.** Quantum-chemical simulation of solvent effects. Tartu, 1993, 110 p.
2. **Peeter Burk.** Theoretical study of gas-phase acid-base equilibria. Tartu, 1994, 96 p.
3. **Victor Lobanov.** Quantitative structure-property relationships in large descriptor spaces. Tartu, 1995, 135 p.
4. **Vahur Mäemets.** The  $^{17}\text{O}$  and  $^1\text{H}$  nuclear magnetic resonance study of  $\text{H}_2\text{O}$  in individual solvents and its charged clusters in aqueous solutions of electrolytes. Tartu, 1997, 140 p.
5. **Andrus Metsala.** Microcanonical rate constant in nonequilibrium distribution of vibrational energy and in restricted intramolecular vibrational energy redistribution on the basis of slater's theory of unimolecular reactions. Tartu, 1997, 150 p.
6. **Uko Maran.** Quantum-mechanical study of potential energy surfaces in different environments. Tartu, 1997, 137 p.
7. **Alar Jänes.** Adsorption of organic compounds on antimony, bismuth and cadmium electrodes. Tartu, 1998, 219 p.
8. **Kaido Tammeveski.** Oxygen electroreduction on thin platinum films and the electrochemical detection of superoxide anion. Tartu, 1998, 139 p.
9. **Ivo Leito.** Studies of Brønsted acid-base equilibria in water and non-aqueous media. Tartu, 1998, 101 p.
10. **Jaan Leis.** Conformational dynamics and equilibria in amides. Tartu, 1998, 131 p.
11. **Toonika Rinken.** The modelling of amperometric biosensors based on oxidoreductases. Tartu, 2000, 108 p.
12. **Dmitri Panov.** Partially solvated Grignard reagents. Tartu, 2000, 64 p.
13. **Kaja Orupõld.** Treatment and analysis of phenolic wastewater with microorganisms. Tartu, 2000, 123 p.
14. **Jüri Ivask.** Ion Chromatographic determination of major anions and cations in polar ice core. Tartu, 2000, 85 p.
15. **Lauri Vares.** Stereoselective Synthesis of Tetrahydrofuran and Tetrahydropyran Derivatives by Use of Asymmetric Horner-Wadsworth-Emmons and Ring Closure Reactions. Tartu, 2000, 184 p.
16. **Martin Lepiku.** Kinetic aspects of dopamine  $\text{D}_2$  receptor interactions with specific ligands. Tartu, 2000, 81 p.
17. **Katrin Sak.** Some aspects of ligand specificity of P2Y receptors. Tartu, 2000, 106 p.
18. **Vello Pällin.** The role of solvation in the formation of iotsitch complexes. Tartu, 2001, 95 p.
19. **Katrin Kollist.** Interactions between polycyclic aromatic compounds and humic substances. Tartu, 2001, 93 p.

20. **Ivar Koppel.** Quantum chemical study of acidity of strong and superstrong Brønsted acids. Tartu, 2001, 104 p.
22. **Viljar Pihl.** The study of the substituent and solvent effects on the acidity of OH and CH acids. Tartu, 2001, 132 p.
23. **Natalia Palm.** Specification of the minimum, sufficient and significant set of descriptors for general description of solvent effects. Tartu, 2001, 134 p.
24. **Sulev Sild.** QSPR/QSAR approaches for complex molecular systems. Tartu, 2001, 134 p.
25. **Ruslan Petrukhin.** Industrial applications of the quantitative structure-property relationships. Tartu, 2001, 162 p.
26. **Boris V. Rogovoy.** Synthesis of (benzotriazolyl)carboximidamides and their application in relations with *N*- and *S*-nucleophiles. Tartu, 2002, 84 p.
27. **Koit Herodes.** Solvent effects on UV-vis absorption spectra of some solvatochromic substances in binary solvent mixtures: the preferential solvation model. Tartu, 2002, 102 p.
28. **Anti Perkson.** Synthesis and characterisation of nanostructured carbon. Tartu, 2002, 152 p.
29. **Ivari Kaljurand.** Self-consistent acidity scales of neutral and cationic Brønsted acids in acetonitrile and tetrahydrofuran. Tartu, 2003, 108 p.
30. **Karmen Lust.** Adsorption of anions on bismuth single crystal electrodes. Tartu, 2003, 128 p.
31. **Mare Piirsalu.** Substituent, temperature and solvent effects on the alkaline hydrolysis of substituted phenyl and alkyl esters of benzoic acid. Tartu, 2003, 156 p.
32. **Meeri Sassian.** Reactions of partially solvated Grignard reagents. Tartu, 2003, 78 p.
33. **Tarmo Tamm.** Quantum chemical modelling of polypyrrole. Tartu, 2003. 100 p.
34. **Erik Teinmaa.** The environmental fate of the particulate matter and organic pollutants from an oil shale power plant. Tartu, 2003. 102 p.
35. **Jaana Tammiku-Taul.** Quantum chemical study of the properties of Grignard reagents. Tartu, 2003. 120 p.
36. **Andre Lomaka.** Biomedical applications of predictive computational chemistry. Tartu, 2003. 132 p.
37. **Kostyantyn Kirichenko.** Benzotriazole — Mediated Carbon–Carbon Bond Formation. Tartu, 2003. 132 p.
38. **Gunnar Nurk.** Adsorption kinetics of some organic compounds on bismuth single crystal electrodes. Tartu, 2003, 170 p.
39. **Mati Arulepp.** Electrochemical characteristics of porous carbon materials and electrical double layer capacitors. Tartu, 2003, 196 p.
40. **Dan Cornel Fara.** QSPR modeling of complexation and distribution of organic compounds. Tartu, 2004, 126 p.
41. **Riina Mahlapuu.** Signalling of galanin and amyloid precursor protein through adenylate cyclase. Tartu, 2004, 124 p.

42. **Mihkel Kerikmäe.** Some luminescent materials for dosimetric applications and physical research. Tartu, 2004, 143 p.
43. **Jaanus Kruusma.** Determination of some important trace metal ions in human blood. Tartu, 2004, 115 p.
43. **Urmas Johanson.** Investigations of the electrochemical properties of polypyrrole modified electrodes. Tartu, 2004, 91 p.
44. **Kaido Sillar.** Computational study of the acid sites in zeolite ZSM-5. Tartu, 2004, 80 p.
45. **Aldo Oras.** Kinetic aspects of dATP $\alpha$ S interaction with P2Y<sub>1</sub> receptor. Tartu, 2004, 75 p.
46. **Erik Mölder.** Measurement of the oxygen mass transfer through the air-water interface. Tartu, 2005, 73 p.
47. **Thomas Thomborg.** The kinetics of electroreduction of peroxodisulfate anion on cadmium (0001) single crystal electrode. Tartu, 2005, 95 p.
48. **Olavi Loog.** Aspects of condensations of carbonyl compounds and their imine analogues. Tartu, 2005, 83 p.
49. **Siim Salmar.** Effect of ultrasound on ester hydrolysis in aqueous ethanol. Tartu, 2006, 73 p.
50. **Ain Uustare.** Modulation of signal transduction of heptahelical receptors by other receptors and G proteins. Tartu, 2006, 121 p.
51. **Sergei Yurchenko.** Determination of some carcinogenic contaminants in food. Tartu, 2006, 143 p.
52. **Kaido Tamm.** QSPR modeling of some properties of organic compounds. Tartu, 2006, 67 p.
53. **Olga Tšubrik.** New methods in the synthesis of multisubstituted hydrazines. Tartu. 2006, 183 p.
54. **Lilli Sooväli.** Spectrophotometric measurements and their uncertainty in chemical analysis and dissociation constant measurements. Tartu, 2006, 125 p.
55. **Eve Koort.** Uncertainty estimation of potentiometrically measured pH and pK<sub>a</sub> values. Tartu, 2006, 139 p.
56. **Sergei Kopanchuk.** Regulation of ligand binding to melanocortin receptor subtypes. Tartu, 2006, 119 p.
57. **Silvar Kallip.** Surface structure of some bismuth and antimony single crystal electrodes. Tartu, 2006, 107 p.
58. **Kristjan Saal.** Surface silanization and its application in biomolecule coupling. Tartu, 2006, 77 p.
59. **Tanel Tätte.** High viscosity Sn(OBu)<sub>4</sub> oligomeric concentrates and their applications in technology. Tartu, 2006, 91 p.
60. **Dimitar Atanasov Dobchev.** Robust QSAR methods for the prediction of properties from molecular structure. Tartu, 2006, 118 p.
61. **Hannes Hagu.** Impact of ultrasound on hydrophobic interactions in solutions. Tartu, 2007, 81 p.
62. **Rutha Jäger.** Electroreduction of peroxodisulfate anion on bismuth electrodes. Tartu, 2007, 142 p.

63. **Kaido Viht.** Immobilizable bisubstrate-analogue inhibitors of basophilic protein kinases: development and application in biosensors. Tartu, 2007, 88 p.
64. **Eva-Ingrid Rõõm.** Acid-base equilibria in nonpolar media. Tartu, 2007, 156 p.
65. **Sven Tamp.** DFT study of the cesium cation containing complexes relevant to the cesium cation binding by the humic acids. Tartu, 2007, 102 p.
66. **Jaak Nerut.** Electroreduction of hexacyanoferrate(III) anion on Cadmium (0001) single crystal electrode. Tartu, 2007, 180 p.
67. **Lauri Jalukse.** Measurement uncertainty estimation in amperometric dissolved oxygen concentration measurement. Tartu, 2007, 112 p.
68. **Aime Lust.** Charge state of dopants and ordered clusters formation in CaF<sub>2</sub>:Mn and CaF<sub>2</sub>:Eu luminophors. Tartu, 2007, 100 p.
69. **Iiris Kahn.** Quantitative Structure-Activity Relationships of environmentally relevant properties. Tartu, 2007, 98 p.
70. **Mari Reinik.** Nitrates, nitrites, N-nitrosamines and polycyclic aromatic hydrocarbons in food: analytical methods, occurrence and dietary intake. Tartu, 2007, 172 p.
71. **Heili Kasuk.** Thermodynamic parameters and adsorption kinetics of organic compounds forming the compact adsorption layer at Bi single crystal electrodes. Tartu, 2007, 212 p.
72. **Erki Enkvist.** Synthesis of adenosine-peptide conjugates for biological applications. Tartu, 2007, 114 p.
73. **Svetoslav Hristov Slavov.** Biomedical applications of the QSAR approach. Tartu, 2007, 146 p.
74. **Eneli Härk.** Electroreduction of complex cations on electrochemically polished Bi(*hkl*) single crystal electrodes. Tartu, 2008, 158 p.
75. **Priit Möller.** Electrochemical characteristics of some cathodes for medium temperature solid oxide fuel cells, synthesized by solid state reaction technique. Tartu, 2008, 90 p.
76. **Signe Viggor.** Impact of biochemical parameters of genetically different pseudomonads at the degradation of phenolic compounds. Tartu, 2008, 122 p.
77. **Ave Sarapuu.** Electrochemical reduction of oxygen on quinone-modified carbon electrodes and on thin films of platinum and gold. Tartu, 2008, 134 p.
78. **Agnes Kütt.** Studies of acid-base equilibria in non-aqueous media. Tartu, 2008, 198 p.
79. **Rouvim Kadis.** Evaluation of measurement uncertainty in analytical chemistry: related concepts and some points of misinterpretation. Tartu, 2008, 118 p.
80. **Valter Reedo.** Elaboration of IVB group metal oxide structures and their possible applications. Tartu, 2008, 98 p.
81. **Aleksei Kuznetsov.** Allosteric effects in reactions catalyzed by the cAMP-dependent protein kinase catalytic subunit. Tartu, 2009, 133 p.

82. **Aleksei Bredihhin.** Use of mono- and polyanions in the synthesis of multisubstituted hydrazine derivatives. Tartu, 2009, 105 p.
83. **Anu Ploom.** Quantitative structure-reactivity analysis in organosilicon chemistry. Tartu, 2009, 99 p.
84. **Argo Vonk.** Determination of adenosine A<sub>2A</sub>- and dopamine D<sub>1</sub> receptor-specific modulation of adenylate cyclase activity in rat striatum. Tartu, 2009, 129 p.
85. **Indrek Kivi.** Synthesis and electrochemical characterization of porous cathode materials for intermediate temperature solid oxide fuel cells. Tartu, 2009, 177 p.
86. **Jaanus Eskusson.** Synthesis and characterisation of diamond-like carbon thin films prepared by pulsed laser deposition method. Tartu, 2009, 117 p.
87. **Margo Lätt.** Carbide derived microporous carbon and electrical double layer capacitors. Tartu, 2009, 107 p.